Molecular Phylogenetics and Evolution 53 (2009) 492–508

Contents lists available at ScienceDirect

Molecular Phylogenetics and Evolution

journal homepage: www.elsevier.com/locate/ympev

Higher-level salamander relationships and divergence dates inferred from complete mitochondrial genomes

Peng Zhang [a,b,*], David B. Wake [a,*]

[a] Department of Integrative Biology, Museum of Vertebrate Zoology, 3101 Valley Life Sciences Building, University of California, Berkeley, CA 94720-3160, USA
[b] Key Laboratory of Gene Engineering of the Ministry of Education, School of Life Sciences, Sun Yat-sen University, Guangzhou 510275, People's Republic of China

ARTICLE INFO

Article history:
Received 19 February 2009
Revised 7 July 2009
Accepted 7 July 2009
Available online 10 July 2009

Keywords:
Salamander
Phylogeny
Mitochondrial genome
Molecular dating

ABSTRACT

Phylogenetic relationships among the salamander families have been difficult to resolve, largely because the window of time in which major lineages diverged was very short relative to the subsequently long evolutionary history of each family. We present seven new complete mitochondrial genomes representing five salamander families that have no or few mitogenome records in GenBank in order to assess the phylogenetic relationships of all salamander families from a mitogenomic perspective. Phylogenetic analyses of two data sets—one combining the entire mitogenome sequence except for the D-loop, and the other combining the deduced amino acid sequences of all 13 mitochondrial protein-coding genes—produce nearly identical well-resolved topologies. The monophyly of each family is supported, including the controversial Proteidae. The internally fertilizing salamanders are demonstrated to be a clade, concordant with recent results using nuclear genes. The internally fertilizing salamanders include two well-supported clades: one is composed of Ambystomatidae, Dicamptodontidae, and Salamandridae, the other Proteidae, Rhyacotritonidae, Amphiumidae, and Plethodontidae. In contrast to results from nuclear loci, our results support the conventional morphological hypothesis that Sirenidae is the sister-group to all other salamanders and they statistically reject the hypothesis from nuclear genes that the suborder Cryptobranchoidea (Cryptobranchidae + Hynobiidae) branched earlier than the Sirenidae. Using recently recommended fossil calibration points and a "soft bound" calibration strategy, we recalculated evolutionary timescales for tetrapods with an emphasis on living salamanders, under a Bayesian framework with and without a rate-autocorrelation assumption. Our dating results indicate: (i) the widely used rate-autocorrelation assumption in relaxed clock analyses is problematic and the accuracy of molecular dating for early lissamphibian evolution is questionable; (ii) the initial diversification of living amphibians occurred later than recent estimates would suggest, from the Late Carboniferous to the Early Permian (~294 MYA); (iii) living salamanders originated during the Early Jurassic (~183 MYA), and (iv) most salamander families had diverged from each other by Late Cretaceous. A likelihood-based ancestral area reconstruction analysis favors a distribution throughout Laurasia in the Early Jurassic for the common ancestor of all living salamanders.

1. Introduction

Salamanders (Caudata), one of three major groups of living amphibians, comprise 578 extant species, most commonly grouped into 67 genera and 10 families (AmphibiaWeb, 2009). Because salamanders are often used as model systems to assess fundamental issues of morphological, developmental and biogeographical evolution, robust phylogenetic hypotheses concerning relationships among the families of living salamanders are basic necessities.

There is a lack of consensus regarding family-level phylogenetic relationships for living salamanders (reviewed in Larson et al., 2003). Most studies support the monophyly of internally fertilizing salamanders, i.e., the families Ambystomatidae, Amphiumidae, Dicamptodontidae, Plethodontidae, Proteidae, Rhyacotritonidae, and Salamandridae (Duellman and Trueb, 1986; Larson and Dimmick, 1993; Hay et al., 1995; Wiens et al., 2005; Roelants et al., 2007), although this conclusion was challenged by three independent studies using both morphological and molecular data (Gao and Shubin, 2001; Weisrock et al., 2005; Frost et al., 2006). Earlier studies placed the family Sirenidae as the sister-group to all remaining salamanders (Goin et al., 1978; Duellman and Trueb, 1986; Milner, 1983, 1988, 2000), but recent analyses of nuclear gene sequences consistently favored the hypothesis that Cryptobranchoidea (Cryptobranchidae and Hynobiidae) branched

* Corresponding authors. Fax: +1 510 643 8238 (D.B. Wake).
E-mail addresses: alarzhang@gmail.com (P. Zhang), wakelab@berkeley.edu (D.B. Wake).

1055-7903/$ - see front matter © 2009 Elsevier Inc. All rights reserved.
doi:10.1016/j.ympev.2009.07.010

earlier than Sirenidae (Wiens et al., 2005; Frost et al., 2006; Roelants et al., 2007). Moreover, relationships within the large clade of internally fertilizing salamanders are not fully resolved and remain controversial.

Salamanders are known to have a long evolutionary age of at least 150 million years (Evans et al., 2005) and their initial diversification likely occurred within a relatively short window of time (Weisrock et al., 2005). When using DNA sequences to infer the phylogeny of salamanders, we face a major problem that the branches grouping multiple families are very short relative to the long terminal branches, which makes the phylogenetic relationships among the families of salamanders difficult to resolve (Wiens et al., 2008). To improve phylogenetic resolution, the most effective method is to increase the amount of phylogenetic signal (i.e., increase the quantity of DNA data). Compared with previous studies that used relatively small amounts of DNA data (Larson and Dimmick, 1993; Hedges and Maxson, 1993; Hay et al., 1995), recent efforts employing increasingly larger quantities of DNA data show better performance for tree resolution and higher levels of congruence with morphological studies (e.g., Roelants et al., 2007).

Timing of phylogenetic events during the evolution history of salamanders has been estimated by earlier workers and is a matter of considerable interest to paleontologists and historical biogeographers. Using mitogenome data but incomplete taxon sampling, Zhang et al. (2005) suggested that the origin of living salamanders was no less than 197 million years ago (MYA). Based on data from the nuclear RAG1 gene, San Mauro et al. (2005) and Hugall et al. (2007) estimated the age of stem Caudata at about 270 million years ago. Another recent molecular study (Roelants et al., 2007), using four nuclear and a mitochondrial marker for representatives of all living families, provided a younger estimate of about 220–249 MYA. Marjanović and Laurin (2007) compiled a supertree including 223 extinct species of lissamphibians. Using paleontological data and inferences, they hypothesized that living salamanders arose in Mid-Late Jurassic (~162 MYA), a much younger date than any calculation based on the molecular data. This apparent discordance on divergence time estimates among different molecular studies and between molecular and fossil results is a focus of our analysis.

Mitochondrial DNA (mtDNA) is a useful marker system in phylogenetic analyses because of its maternal mode of inheritance and relative lack of recombination (Saccone et al., 1999). As a single, haploid, nonrecombining linkage unit, the mt genome of vertebrates represents only one-fourth of the effective population size compared with the nuclear (nc) genome, which results in a shorter expected coalescence time for mt loci compared with nc loci and a greater probability that the mt gene tree will accurately reflect the species tree (Moore, 1995). Moreover, mtDNA is a moderate-scale genome suitable for complete sequencing and thus provides substantial amounts of DNA data for phylogenetic analyses. Previous studies demonstrated that mitogenomic data recovered robust phylogenies (with high statistical support) for many taxa (Miya and Nishida, 2000; Miya et al., 2001; Mueller et al., 2004; Zhang et al., 2005, 2006), and thus may resolve questions of higher-level relationships of salamanders.

In order to re-examine the family-level relationships among living salamanders, we sequenced seven complete mitochondrial genomes of salamanders from five families, four previously not represented. By combining these sequences with published salamander mitochondrial genomes, we present a comprehensive molecular phylogenetic analysis for living salamanders. We also use various statistical tests to evaluate alternative phylogenetic hypotheses derived from previous studies as well as the hypotheses generated from our new phylogenetic results. Finally, we present estimates for the time tree of evolution in this clade using new analytical methods.

2. Materials and methods

2.1. Taxon sampling for mitochondrial genomes

Complete mitochondrial genomes for 83 salamanders were deposited in GenBank before this study began, representing 6 of 10 families. Our sampling strategy is to include all extant salamander families but also all key genera for each family, in order to reduce long-branch attraction and to more accurately date phylogenetic events. For the Plethodontidae, Salamandridae, Hynobiidae, Ambystomatidae, and Rhyacotritonidae, existing data deposited in GenBank are relatively abundant. For the Cryptobranchidae, the sole North American species, *Cryptobranchus alleganiensis,* was added to the Asian species of *Andrias* (previously studied). For the remaining families (Amphiumidae, Dicamptodontidae, Proteidae, and Sirenidae), we added species to include a total of six missing genera. Moreover, complete mitochondrial genomes of three frogs, three caecilians, one lungfish and one coelacanth were retrieved from GenBank to serve as outgroup taxa in the phylogenetic analyses. Data for four representative sauropsids (1 bird, 1 lizard, and 2 crocodiles) were retrieved from GenBank to be used in our molecular dating analyses. The details for all sequences used in this study are given in Table 1.

2.2. Laboratory protocols

Total DNA was purified from frozen or ethanol-preserved tissues (liver or muscle) using the Qiagen (Valencia, CA) DNeasy Blood and Tissue Kit. A suite of 22 primers (Table 2) was used to amplify contiguous and overlapping fragments that covered the entire mt genome (Fig. 1). PCRs were performed with AccuTaq LA DNA Polymerase (SIGMA) in total volumes of 25 μl, using the following cycling conditions: an initial denaturing step at 96 °C for 2 min; 35 cycles of denaturing at 94 °C for 15 s, annealing at 45–55 °C (see Table 2) for 60 s, and extending at 72 °C for 5 min; and a final extending step of 72 °C for 10 min. PCR products were purified either directly via ExoSAP (USB) treatment or gel-cutting (1% TAE agarose) using the gel purification kit (Qiagen). Sequencing was performed directly with the corresponding PCR primers using the BigDye Deoxy Terminator cycle-sequencing kit v3.1 (Applied Biosystems) in an automated DNA sequencer (ABI PRISM 3730) following the manufacturer's instructions. For some large PCR fragments, specific primers were designed according to newly obtained sequences to facilitate primer walking.

2.3. Sequence alignments, data partition, and model selection

We included all species listed in Table 1 except for the 4 sauropsid species (33 in total) for phylogenetic reconstruction. For estimates of divergence dates, all species (37 in total) were used. Ribosomal RNAs and tRNAs were aligned manually with reference to secondary structure, according to recommendations of Kjer (1995) and Gutell et al. (1994). Models for rRNA secondary structure came from the Comparative RNA Web (CRW) site. Length variable regions (mainly rRNA and tRNA loops) were excluded. All 22 tRNA alignments were then combined to generate a concatenated alignment. Several tRNA genes are incomplete in some mt genomes. For these, "Ns" were added to the corresponding alignments and treated as missing data. All 13 protein-coding genes were translated to amino acids and aligned using Clustal W (Thompson et al., 1997) implemented in the Megalign program (DNASTAR package) at default settings, and then shifted back to DNA sequences. Thus we obtained alignments for amino acids and nucleotides simultaneously. To avoid bias in refining the protein-coding gene alignments, we used Gblocks (Castresana, 2000) to extract

Table 1
List of species used in this study, along with GenBank accession numbers and vouchers (if applicable).

Taxonomy	Species	Voucher	GenBank No.	Reference (for Caudata only)
Coelacanthiformes	*Latimeria chalumnae*	—	NC_001804	
Dipnoi	*Protopterus dolloi*	—	NC_001708	
Amniote	*Takydromus tachydromoides*	—	NC_008773	
	Gallus gallus	—	NC_001323	
	Alligator mississippiensis	—	NC_001922	
	Caiman crocodilus	—	NC_002744	
Anura	*Bombina fortinuptialis*	—	AY458591	
	Xenopus tropicalis	—	NC_006839	
	Pelobates cultripes	—	NC_008144	
Gymnophiona	*Typhlonectes natans*	—	NC 002471	
	Ichthyophis bannanicus	—	AY458594	
	Rhinatrema bivittatum	—	NC_006303	
Caudata				
Ambystomatidae	*Ambystoma tigrinum*	—	NC_006887	Samuels et al. (2005)
	Ambystoma mexicanum	—	AJ584639	Arnason et al. (2004)
Amphiumidae	*Amphiuma means*[*]	RMB2489	GQ368656	This study
Cryptobranchidae	*Andrias davidianus*	—	AJ492192	Zhang et al. (2003a)
	Cryptobranchus alleganiensis	No voucher	GQ368662	This study
Dicamptodontidae	*Dicamptodon aterrimus*	MVZ228774	GQ368657	This study
Hynobiidae	*Onychodactylus fischeri*	—	NC_008089	Zhang et al. (2006)
	Hynobius amjiensis	—	NC_008076	Zhang et al. (2006)
	Ranodon sibiricus	—	NC_004021	Zhang et al. (2003b)
	Batrachuperus tibetanus	—	NC_008085	Zhang et al. (2006)
Plethodontidae	*Aneides hardii*	—	NC_006338	Mueller et al. (2004)
	Batrachoseps attenuatus	—	NC_006340	Mueller et al. (2004)
	Eurycea bislineata	—	NC_006329	Mueller et al. (2004)
	Pseudotriton ruber	—	NC_006332	Mueller et al. (2004)
	Plethodon petraeus	—	NC_006334	Mueller et al. (2004)
Proteidae	*Necturus beyeri*	MVZ187709	GQ368658	This study
	Proteus anguinus	MVZ244076	GQ368659	This study
Rhyacotritonidae	*Rhyacotriton variegatus*	—	NC_006331	Mueller et al. (2004)
Salamandridae	*Taricha granulosa*	—	EU880333	Zhang et al. (2008)
	Salamandrina terdigitata	—	EU880332	Zhang et al. (2008)
	Mertensiella caucasica	—	EU880319	Zhang et al. (2008)
	Salamandra salamandra	—	EU880331	Zhang et al. (2008)
	Tylototriton asperrimus	—	EU880340	Zhang et al. (2008)
Sirenidae	*Siren intermedia*[*]	RMB3124	GQ368661	This study
	Pseudobranchus axanthus[*]	RMB3228	GQ368660	This study

[*] Complete mtDNA sequences except for a portion of the control region.

Table 2
Primers used to amplify the complete salamander mitochondrial genomes (see Fig. 1 to trace fragments along the genome).

Fragment name	Primer name	Sequence (5′—3′)	Approximate product length (bp)	Annealing temperature (°C) used in the PCR
L1	12SAL	AAACTGGGATTAGATACCCCACTAT	1500	55
	16S2000H	GTGATTAYGCTACCTTTGCACGGT		
L2	LX12SN1	TACACACCGCCCGTCA	1600	55
	LX16S1R	GACCTGGATTACTCCGGTCTGAACTC		
A	LX16S1	GGTTTACGACCTCGATGTTGGATCA	1500	55
	Met3850H	GGTATGGGCCCAARAGCTT		
B	Ile3700L	AGGRRYYACTTTGATARAGT	1600	55
	COI5350H	AGGGTGCCRATRTCYTTRTGRTT		
C	Asn5100L	GACCTTTTAGTTAACAGCTAAA	1800	45
	Asp6900H	ACAAGGAATTGTAATIGTTTTACTAA		
E	Ser6800L	GAACCCCCITARRYTAATTTCAAGT	900	50
	Lys7700H	CACCGRTCTWYAGCTTAAAAGGC		
F	Lys7700L	AAGCAATAGCCTTTTAAGC	2100	50
	Arg9820H	AACCRAAATTTAYTRAGTCGAAAT		
G	Arg9820L	ATTTCGACTYAGTAAATTTYGGTT	1900	50
	Leu11720H	CATTACTTTTACTTGGRNTTGCACC		
H	His11560L	AAAATWNTAGATTGTGRTTCTA	1200	45
	ND512800H	CCYATTTTTCGRATRTCYTGYTC		
I	ND512680L	ACATCCAGYCARYTAGGIYTAATAATAGT	1800	45
	CB14530H	GCICCTCARAATGATATTTGTCC		
M	Glu14100L	GAAAAACCAAYGTTGTATTCAACTATAA	Variable	50
	12S600H	TCGATTATAGAACAGGCTCCTCT	>2700	

regions of defined sequence conservation from the alignments. We used a relative stringent parameter setting: minimum number of sequences for a conserved position 28; minimum number of sequences for a flanking position 33; maximum number of contiguous nonconserved positions 8; minimum length of a block 10 (under the codon mode). Finally, a DNA dataset combining all 16 DNA alignments (2 rRNA, 1 tRNAs and 13 protein genes) and a protein dataset combining all 13 protein alignments were generated. The DNA

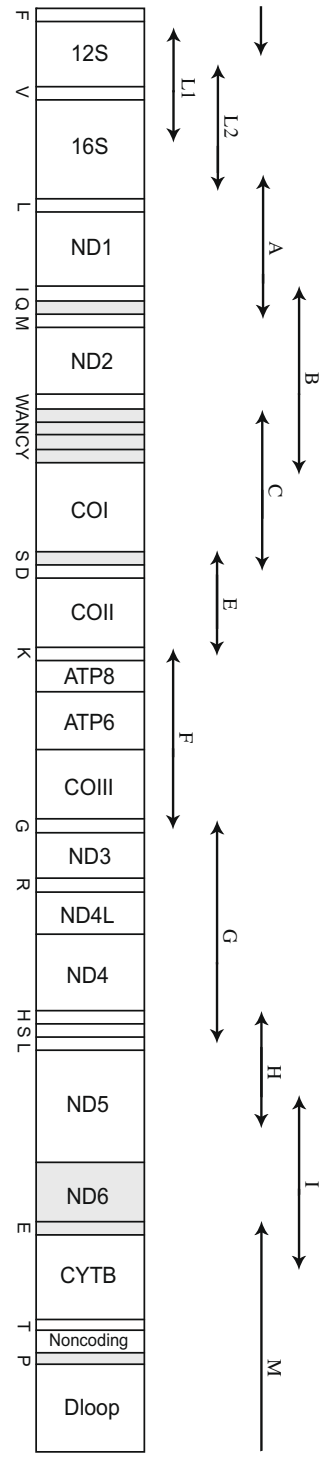

Fig. 1. Gene organization and sequencing strategy for mt genomes of salamanders. Genes encoded by the L strand are shaded. Arrow headed segments denote the location of the fragments amplified by PCR with each pair of primers (see Table 2 for the primer DNA sequence associated with each fragment).

dataset was divided into 42 partitions according to genes and codon positions (tRNAs, 2 rRNAs, every codon position for 13 protein genes). Model selection for each partition was made according to the Akaike information criterion (AIC) as implemented in MrModelTest 2.2 (http://www.ebc.uu.se/systzoo/staff/nylander.html). The best fitting model for each partition was used in subsequent Bayesian phylogenetic analyses. A substitution saturation test (Xia et al., 2003) for all 42 partitions was performed using DAMBE version 4.5.33 (Xia and Xie, 2001).

2.4. Phylogenetic analyses

Maximum parsimony (MP) analyses were performed both on the DNA and the protein datasets using PAUP* 4.0b10 (Swofford, 2001). MP analyses were conducted using heuristic searches (TBR branch swapping; MULPARS option in effect) with 100 random-addition sequences. All sites were given equal weight in the parsimony analysis. Support for internal branches in the parsimony analysis was assessed using 1000 bootstrap replicates, with 10 random-addition sequences performed in each replication.

Maximum-likelihood (ML) phylogenetic analyses were performed on the DNA dataset using PAUP* 4.0b10 with a heuristic search option and stepwise addition of taxa, 10 random-addition replicates, and TBR branch swapping. The nucleotide substitution model selection was carried out using ModelTest version 3.7 Posada and Crandall, 1998), applying the Akaike information criterion. The resulting models and estimated parameters were used in the ML analyses. The protein ML analyses were conducted using PHYML version 2.4.4 (Guindon and Gascuel, 2003). A BIONJ tree was used as a starting tree to search for the ML tree with the mtREV + I + Γ model. Robustness of the phylogenetic results was tested by bootstrap analyses with 1000 replicates, or aLRT SH-like method (Anisimova and Gascue, 2006; as implemented in PHYML-aLRT version 1.1).

The DNA dataset was also subjected to Bayesian inference using MRBAYES version 3.1.2 (Huelsenbeck and Ronquist, 2001), under a partitioning strategy. The dataset was divided into 42 partitions: two rRNAs, the concatenated tRNAs, and every codon position of 13 protein-coding genes. The best-fitting nucleotide substitution models for each of the 42 partitions were selected using the hierarchical likelihood ratio test implemented in MRMODELTEST version 2.2. (http://www.ebc.uu.se/systzoo/staff/nylander.html). Metropolis-coupled Markov chain Monte Carlo (MCMC) analyses (with random starting trees) were run with one cold and three heated chains (temperature set to 0.1) for 20 million generations and sampled every 1000 generations. The burn-in parameter was empirically estimated by plotting-ln *L* against the generation number using Tracer version 1.3 (http://evolve.zoo.ox.ac.uk/beast/help/Tracer), and the trees corresponding to the first 5–7 million generations were discarded. To ensure that our analyses were not trapped in local optima, four independent MCMC runs were performed. Topologies and posterior clade probabilities from different runs were compared for congruence.

Tests of alternative phylogenetic hypotheses among living salamanders were conducted in an ML framework using the CONSEL program (Shimodaira and Hasegawa, 2001). The first step was to reconstruct alternative tree topologies. PAUP* heuristic searches under a GTR + I + Γ model and incorporating a topological constraint were conducted in order to identify the highest-likelihood topology that satisfied a given hypothesis. Second, PAUP* (or PAML; Yang, 1997) was used to produce a log file for the site-wise log-likelihoods of alternative trees given the concatenated data set with a GTR + I + Γ model (or mtREV + I + Γ model for protein data). The generated log file was run in CONSEL to calculate the *p*-value for each alternative topology using the approximately unbiased (AU) test (Shimodaira, 2002) and the Kishino–Hasegawa (KH) test (Kishino and Hasegawa, 1989).

2.5. Molecular dating

The use of multiple calibration points is expected to provide overall more realistic divergence time estimates than using a single point or only a few such points, which are likely to result in high estimation errors for distantly related nodes (Müller and Reisz, 2005). The extensive use of the 'mammal–bird split' for calibration recently culminated in an open debate involving both

paleontologists and molecular biologists (Graur and Martin, 2004; Müller and Reisz, 2005). For external calibration points outside the amphibian lineages, we decided to use some recently advocated calibration points: the Lungfish–Tetrapod split (408–419 MYA; Müller and Reisz, 2005), Amphibia–Amniota split (330–360 MYA; derived from Benton and Donoghue, 2007; Marjanović and Laurin, 2007), Bird–Lizard split (252–300 MYA; from Müller and Reisz, 2005; Benton and Donoghue, 2007), Bird–Crocodile split (235–251 MYA; from Müller and Reisz, 2005; Benton and Donoghue, 2007) and Alligator–Caiman split (66–75 MYA; Müller and Reisz, 2005). The use of internal and external, as well as both young and old calibration points has recently been advocated by paleontologists (Brochu, 2004; Marjanović and Laurin, 2007). In order to examine this issue, we constrained five nodes as minimum dates in addition to those already selected, based on known fossil dates: the common ancestor of salamanders and frogs was constrained to be at least 250 MYA (*Triadobatrachus massinoti*, Rage and Rocek, 1989; *Czatkobatrachus polonicus*, Evans and Borsuk-Białynicka, 1998); the origin of crown-group salamanders was constrained to be at least 151 MYA (*Iridotriton hechti*, Evans et al., 2005); the split between cryptobranchid and hynobiid salamanders was constrained to be at least 145 MYA (*Chunerpeton tianyiense*, Gao and Shubin, 2003), which is a more conservative minimum age for this problematic fossil than the original assumption of a Middle Jurassic age by Gao and Shubin; the *Ambystoma–Dicamptodon* split was constrained to be at least 55.8 MYA (*Dicamptodon antiquus* from the late Paleocene, Naylor and Fox, 1993); and the *Necturus–Proteus* split was constrained to be at least 55.8 MYA (*Necturus krausei* from Late Paleocene, Estes, 1981). A total number of 15 constraints were used in this analysis (abbreviated as 15C).

Marjanović and Laurin (2007) argued the necessity for the use of maximal constraints within amphibian lineages when performing molecular dating, and suggested some calibration points with both maximal and minimal bounds within Lissamphibia. Because the lissamphibian fossil record is rather poor, using maximal bounds based on poor fossil records is risky. However, to compare molecular estimates from different constraint combinations, we included two suggested maximal bounds: 275 MYA for Batrachia (frog–salamander split) and 170 MYA for Caudata (origin of living salamanders) (Marjanović and Laurin, 2007). A total of 17 constraints were used in this analysis (abbreviated as 17C).

Bayesian inference under various relaxed-clock models, implemented by Multidivtime (Thorne and Kishino, 2002) and BEAST v1.4.5 (Drummond et al., 2006), was used to perform the molecular dating process. We did not use the penalized likelihood method implemented in R8S (Sanderson, 2003) because that method uses only phylogenetic topology and branch length information derived from third-party programs and is unable to perform a "multiple-loci" analysis.

All third codon positions were excluded from our datasets because these saturated sites are likely to bring misleading effects on branch length estimation. Because the fit of the substitution model to the data is better when the data set is partitioned by codon position than by gene (Mueller et al., 2004), we partitioned our DNA dataset as follows: separate partitions for each of the two ribosomal RNAs, the concatenated tRNAs, separate partitions for all first codon positions and all second codon positions of protein coding genes.

In the Multidivtime analyses, optimized branch lengths with their variance–covariance matrices of the DNA dataset were estimated for each partition with the program Estbranches_dna, using an F84 + G model with parameters estimated by PAML (Yang, 1997). The coelacanth sequence (*Latimeria chalumnae*) served as the outgroup allowing the tree relating the remaining 36 ingroup sequences to be rooted. The priors for the mean and standard deviation of the ingroup root age (Lungfish–Tetrapod split, 408–419 MYA; Müller and Reisz, 2005), rttm and rttmsd were set to equivalents of 413 million years and 5 million years (i.e., rttm = 4.13, rttmsd = 0.05), respectively. The prior mean and standard deviation for the Gamma distribution describing the rate at the root node (rtrate and rtratesd) were both set to 0.1. These values were based on the median of the substitution path lengths between the ingroup root and each terminal, divided by rttm (as suggested by the author). The prior mean and standard deviation for the Gamma distribution of the parameter controlling rate variation over time (i.e. brownmean and brownsd) were both set to 0.5. To allow the Markov chain to reach stationarity, the Markov chain Monte Carlo algorithm completed 200,000 initial cycles before the state of the Markov chain was sampled. Thereafter, the Markov chain was sampled every 100 cycles until a total of 10,000 samples was collected. To test whether or not the Markov chain was converging, three single runs were performed. Similar results from the three runs were observed.

In the BEAST analyses, the uncorrelated lognormal model was used to describe the relaxed clock, while GTR + I + Γ was used to describe the substitution model for five partitions of the dataset. The Yule process was used to describe speciation. The consensus tree obtained from phylogenetic analyses was used as the input topology. Yang and Rannala (2006) argued that using a rigid calibration constraint is likely to result in estimates of divergence times with artificial precision; a "soft" calibration constraint should be used whenever possible. Accordingly, we were concerned with the use of maximal bounds in our molecular dating process, because problematic maximal constraints will strongly influence our dating results. To this end, besides the conventional uniform calibration strategy, we also used lognormal distributions to describe the priors of those calibration points with maximum boundaries, representing a "soft" calibration strategy. The means and standard deviations of the lognormal distribution for each calibration point were chosen so that 95% of the probability lies within the minimum bound and the maximum bound and the means are the arithmetical medians of the intervals. This "soft" bound strategy allows sampling time estimates beyond maximal bounds with 5% probability during Bayesian MCMC chains, which will depress the influence from problematic constraints to some extent. A test MCMC run with 10^6 generations was first performed to optimize the scale factors of the priori function. For every single analysis, the final MCMC chain was run twice for 100 million generations sampled every 1000 generations. Burn-in and convergence of the chains were determined with Tracer 1.3 (Drummond et al., 2006). The measures of effective sample sizes (ESS) were used to determine the Bayesian statistical significance of each parameter. For the sake of computational cost, our BEAST time analyses were only run for nodes of special concern (see relevant tables and figures).

2.6. Historical biogeography reconstruction

While there is little doubt concerning the Laurasian origin for living salamanders because nearly all fossil and extant species occur in the Northern Hemisphere, their ancestral distribution ranges, routes and directions for dispersal are not clear. To reconstruct the historical biogeographic scenarios for living salamanders, ancestral geographic ranges for nodes along the salamander phylogeny were explored with Lagrange 1.0 (Ree et al., 2005). This method was preferred instead of a dispersal-vicariance analysis, as implemented in DIVA (Ronquist, 1997), because it takes into account more realistic parameters including divergence time estimates, dispersal capacities and extinction rates, and paleogeographic information between regions in geologic time.

We used the salamander portion of the time tree generated by the molecular dating analyses as the input time-calibrated

phylogeny and treated the terminal species as genera. Therefore, the distribution of a terminal taxon does not represent the species but the genus. Moreover, in addition to the distribution of living species, we took into account the fossil distribution of each genus (data from Estes, 1981). According to the current distribution pattern of salamanders, we divided the Laurasian landmass into four areas: western North America (WN), eastern North America (EN), eastern Eurasia (EE) and western Eurasia (WE). We parameterized connections between the four areas as follows. The Turgai sea separated EE from WE at least from the Middle Jurassic (160 MYA) to the Oligocene (29 MYA) (Briggs, 1995), although connections were suggested for plants during the last 50 MYA (Ree et al., 2005). Therefore we set the probability of dispersal success to zero 160–50 MYA and one over this period. Between WN and EN, the probability was zero during the Cretaceous (110–70 MYA) (blocked by epicontinental seaway), and one over this period (Steven, 1999). Between WE and EN (connected through the North Atlantic land bridge), the probability was one until 25 MYA, then declined linearly to zero at 15 MYA (Manchester, 1999; Tiffney, 2000). Between WN and EE (connected through the Bering land bridge), the probability was one until 5 MYA, and zero thereafter (Tiffney, 2000). To optimize two parameters, dispersal capacity (λ_D) and extinction rate (λ_E), following Ree et al. (2005), we performed several analyses with low and high rate scenarios of dispersal and extinction. Different combinations of λ_D and λ_E were explored in the high rate scenario, ranging from λ_D, λ_E = 0.01 to 0.09, although low rate scenarios were explored ranging from λ_D, λ_E = 0.001 to 0.009. For each combination of parameter values, 10^4 simulations were run to obtain overall likelihood values. The highest overall likelihood was obtained at a low rate of dispersal and extinction, where λ_D = 0.007 and λ_E = 0.001. Once optimal λ_D and λ_E were determined, 10^5 simulations were run to obtain the final result. The statistical significance of likelihood differences between biogeographic scenarios was assessed using the conventional cutoff value of two log-likelihood units (Edwards 1992). For most nodes, Lagrange gave more than one possible biogeographic scenario, but we only reported the one with the highest likelihood value. The statistical support for a certain reported scenario is the relative probability (fraction of the global likelihood).

3. Results

3.1. Protein phylogeny

The protein data set that combines all 13 protein-coding mitochondrial genes contains 3423 characters with 1495 constant positions, 451 uninformative positions, and 1477 parsimony-informative positions. Parsimony analysis of the combined data gives a single tree 12217 steps in length (RI = 0.4165, CI = 0.4734; Fig. 2). However, branch support for many nodes in the MP tree

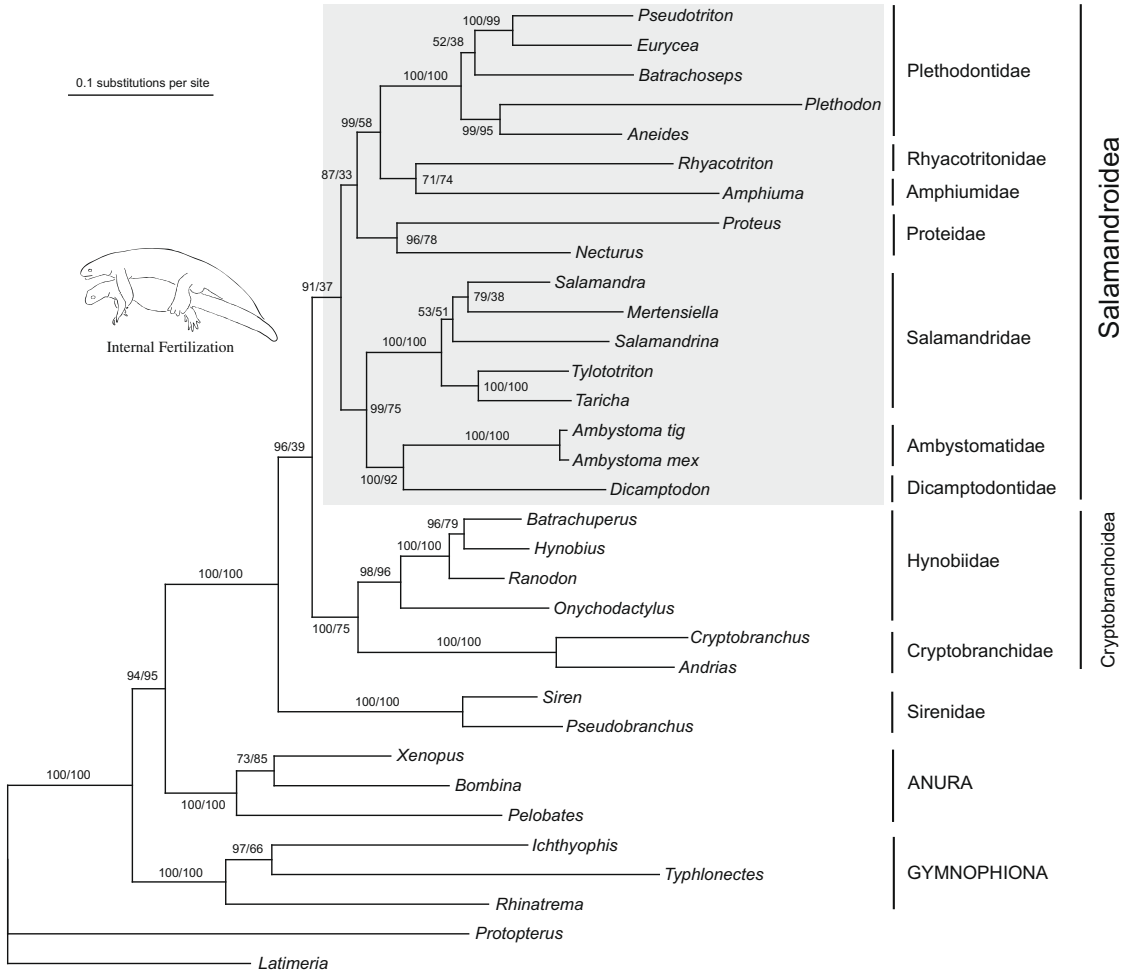

Fig. 2. Salamander phylogeny based on parsimony and maximum-likelihood analyses of mitochondrial protein dataset that combines all 13 protein sequences deduced from complete mitochondrial genomes. The ML topology is identical to the parsimony topology, and their branch-support measures are mapped to the phylogram. Left numbers along branches represent maximum-likelihood bootstrap values and right numbers represent parsimony bootstrap values. Branch lengths were estimated by maximum-likelihood inference. All salamanders with internally fertilizing reproduction mode are shaded.

is weak (bootstrap <50%). Maximum likelihood analysis of the protein data using a mtREV + I + Γ model produces an identical topology ($\ln L = -67251.17$) as that found in parsimony but receives higher statistical support for most nodes (Fig. 2). In both MP and ML analyses, the protein tree provides strong support for several conventional groupings: monophyly of living amphibians, frogs, salamanders, and caecilians, and a sister-taxon relationship of frogs and salamanders (the Batrachia hypothesis). The monophyly of seven families (Sirenidae, Cryptobranchidae, Hynobiidae, Salamandridae, Amystomatidae, Proteidae, and Plethodontidae), is strongly supported by ML analysis. As to salamander phylogeny, the sister-taxon relationship of Hynobiidae and Cryptobranchidae (Cryptobranchoidea) is strongly supported by ML analysis (BS = 100%). Sirenidae is placed basally among the salamanders, followed by Cryptobranchoidea. Monophyly of the internally fertilizing (a derived trait, see below) salamander families (usually termed Salamandroidea) is strongly supported by ML analysis (BS = 91%). The Salamandroidea contains two distinct clades: (1) Salamandridae + Dicamptodontidae + Ambystomatidae; the sister-taxon relationship of Ambystomatidae and Dicamptodontidae is strongly supported both by MP and ML (BS > 90%). Placement of Salamandridae as the sister taxon to the ambystomatid-dicamptodontid clade also receives strong support from ML analysis (BS = 99%). (2) Plethodontidae + Amphiumidae + Rhyacotritonidae + Proteidae. Nodal support for a clade composed of Amphiumidae and Rhyacotritonidae is moderate (BS ~70%); its sister taxon is Plethodontidae. Proteidae is the sister-group of the clade formed by Plethodontidae + Amphiumidae + Rhyacotritonidae.

3.2. DNA phylogeny

The DNA data set combining two rRNAs, the concatenated tRNAs, and 13 protein-coding gene alignments contains 12794 characters (4844 constant, 1091 uninformative variable, and 6859 parsimony-informative). The saturation test on 42 partitions of the DNA alignment (2 rRNAs, tRNAs, and each codon position for 13 protein genes) is summarized in Table 3. Unsurprisingly, third codon positions of all mitochondrial protein genes are subject to strong substitution saturation and show poor performance in phylogenetic reconstructions since the salamanders are an old lineage. Therefore, the DNA dataset (large dataset) was also analyzed with all third codon positions excluded (small dataset); this new DNA dataset contains 9554 positions with 4070 parsimony-informative sites. The best-fit substitution model for the small dataset selected by the Akaike Information Criterion embedded in ModelTest is GTR + I + Γ. Maximum likelihood analysis of the small data set yields a well-resolved topology ($\ln L = -109113.27$; Fig. 3) only slightly different from the protein tree. Four independent partitioned Bayesian analyses of the small dataset produce identical topologies and similar posterior probability support levels, in full congruence with the ML tree.

The PAUP* heuristic maximum likelihood analysis on the DNA data set without exclusion (large dataset) gives a different topology ($-\ln L = 217842.73$; result not shown) to that found in the small dataset. However, when we calculated the likelihood values for the small dataset topology based on the large dataset, we found that the topology inferred from the small dataset has higher maximum-likelihood value than the best tree found by PAUP* ($-\ln L = 217836.02$ vs $-\ln L = 217842.73$). It seems that the PAUP* heuristic ML search on the large dataset is incomplete and likely trapped by local likelihood peaks. Because the heuristic ML search on the large dataset is likely subject to a local-optima trap, it is difficult to perform a bootstrap analysis for this dataset. We therefore use the SH-like aLRT test as an alternative to bootstrapping. The SH-like aLRT test gives similar results to bootstrapping in most cases (Anisimova and Gascue, 2006). Remarkably, four independent partitioned Bayesian analyses of the large dataset produce the identical topology as that found by the small dataset, which implies that the partitioned Bayesian analysis is more reliable than the heuristic maximum likelihood analysis when handing highly heterogenous data.

The phylogenies determined both by large and small datasets are all well resolved (Fig. 3); support for most branches is 0.9–1.0 (ML bootstrap, Bayesian PP, and aLRT). The phylogenetic relationships among living salamanders recovered by DNA data sets show only slight differences from the protein phylogeny: (1) the DNA results support a relationship of ((Amphiumidae, Plethodontidae), Rhyacotritonidae) (Fig. 3. node s) while the protein tree favors ((Amphiumidae, Rhyacotritonidae), Plethodontidae); (2) Within Salamandridae, the DNA trees place *Salamandrina* as the basal branch (Fig. 3. node o) instead of grouping it with "true" salamanders (*Salamandra* and *Mertensiella*), as in the protein tree. Because

Table 3
Model parameters and saturation test result for each data partition. Gene abbreviations as followed: ATP6_1 represents all first codon positions of ATP6 gene, ATP6_2 represents all second codon positions of ATP6 gene, and so on. Saturated results are shaded.

Partitions	Best model	Proportion of invariable sites	Gamma	Saturation test result	Partitions	Best model	Proportion of invariable sites	Gamma	Saturation test result
12S	GTR + I + Γ	0.2746	0.7321	Little	CYTB_2	GTR + I + Γ	0.4860	0.4567	Little
16S	GTR + I + Γ	0.3068	0.8156	Little	ND1_2	GTR + I + Γ	0.5472	0.5326	Little
tRNAs	GTR + I + Γ	0.1362	0.8616	Little	ND2_2	GTR + I + Γ	0.3868	0.9969	Little
ATP6_1	GTR + I + Γ	0.2873	0.4967	Little	ND3_2	GTR + I + Γ	0.5995	0.6676	Little
ATP8_1	HKY + I	0.3698	–	Substantial	ND4_2	GTR + I + Γ	0.5106	0.9084	Little
COI_1	SYM + I + Γ	0.6383	1.3706	Little	ND4L_2	GTR + Γ	–	0.2923	Little
COII_1	GTR + I + Γ	0.4616	1.0143	Little	ND5_2	GTR + I + Γ	0.3462	0.5378	Little
COIII_1	GTR + I + Γ	0.5394	1.0301	Little	ND6_2	GTR + Γ	–	0.4282	Little
CYTB_1	GTR + I + Γ	0.4321	0.6022	Little	ATP6_3	GTR + I + Γ	0.0204	0.7206	Useless
ND1_1	GTR + I + Γ	0.4360	1.2895	Little	ATP8_3	HKY + Γ	–	0.5722	Substantial
ND2_1	GTR + I + Γ	0.2731	1.3784	Little	COI_3	GTR + Γ	–	0.2162	Very poor
ND3_1	GTR + I + Γ	0.4294	0.9351	Little	COII_3	GTR + I + Γ	0.0063	0.5564	Very poor
ND4_1	GTR + I + Γ	0.3577	1.2672	Little	COIII_3	GTR + I + Γ	0.0114	0.3146	Very poor
ND4L_1	SYM + Γ	–	0.4579	Little	CYTB_3	GTR + Γ	–	0.3738	Useless
ND5_1	GTR + I + Γ	0.3470	1.0237	Little	ND1_3	GTR + Γ	–	0.6114	Useless
ND6_1	GTR + I + Γ	0.1184	0.7516	Little	ND2_3	GTR + Γ	–	0.7612	Useless
ATP6_2	GTR + I + Γ	0.4076	0.4262	Little	ND3_3	HKY + Γ	–	0.4007	Useless
ATP8_2	HKY + I	0.3806	–	Little	ND4_3	GTR + Γ	–	0.5923	Useless
COI_2	GTR + I + Γ	0.7760	0.9037	Little	ND4L_3	GTR + I + Γ	0.0149	0.9606	Useless
COII_2	GTR + I + Γ	0.5048	0.9148	Little	ND5_3	GTR + Γ	–	0.5049	Useless
COIII_2	GTR + I + Γ	0.6244	0.5140	Little	ND6_3	GTR + I + Γ	0.0149	0.8482	Useless

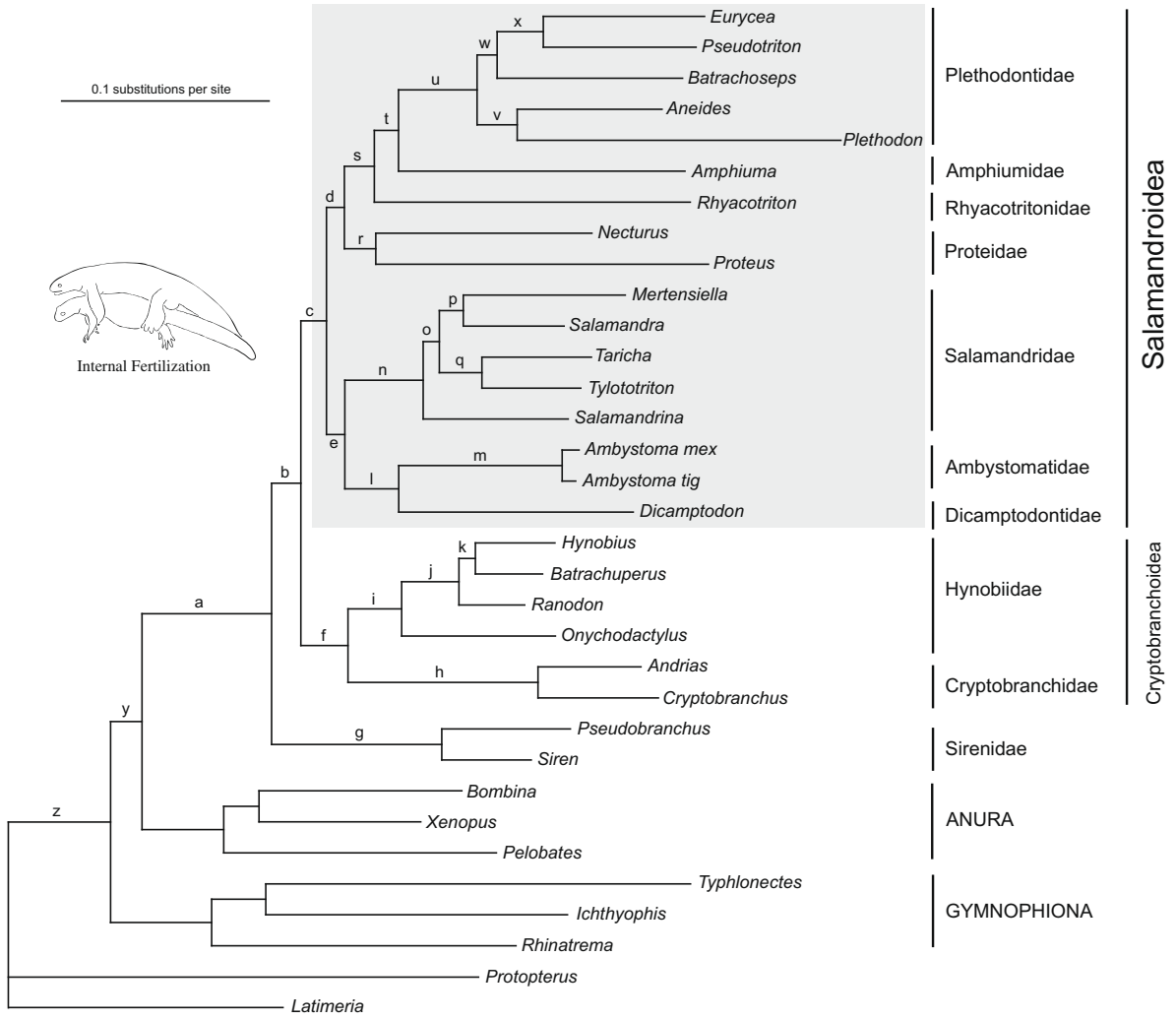

	a	b	c	d	e	f	g	h	i	j	k	l	m	n	o	p	q	r	s	t	u	v	w	x	y	z
ML BS (E3)	100	98	100	100	100	100	100	100	100	100	85	100	100	100	87	100	100	96	100	93	100	100	81	100	88	100
BI PP (E3)	1.0	1.0	1.0	1.0	1.0	1.0	1.0	1.0	1.0	1.0	1.0	1.0	1.0	1.0	1.0	1.0	1.0	1.0	1.0	1.0	1.0	1.0	1.0	1.0	1.0	1.0
aLRT (ALL)	1.0	0.91	1.0	0.99	0.98	1.0	1.0	1.0	1.0	1.0	0.98	1.0	1.0	1.0	0.99	1.0	1.0	0.98	1.0	0.9	1.0	1.0	0.13	1.0	0.92	1.0
BI PP (ALL)	1.0	1.0	1.0	1.0	1.0	1.0	1.0	1.0	1.0	1.0	1.0	1.0	1.0	1.0	1.0	1.0	1.0	1.0	1.0	1.0	1.0	1.0	1.0	1.0	1.0	1.0

Fig. 3. Phylogenetic relationships of living salamanders inferred from mitochondrial genome sequences. The DNA dataset was analyzed with (ALL) or without (E3) all third codon positions. Branches with letters have branch support values given below the tree for maximum likelihood bootstrapping (ML BS), aLRT test values (aLRT), and Bayesian posterior probabilities (BI PP). Branch lengths were from maximum-likelihood analysis on the dataset excluding all 3rd codon positions. All salamanders with internally fertilizing reproduction mode are shaded.

the branch supports for these questionable nodes in the protein phylogeny are either moderate (Amphiumidae + Rhyacotritonidae, ML bootstrap ~70%) or weak (*Salamandrina* + true salamanders, ML bootstrap ~50%), and the DNA results are also supported by previous studies (Roelants et al., 2007; Zhang et al., 2008), we consider the DNA phylogeny to be more reliable.

Parsimony analyses of both the large and the small DNA data sets produce very different topologies with respect to the DNA ML tree (results not shown). In the MP tree inferred from the small dataset, the European proteid, *Proteus anguinus*, is the sister taxon to a group containing all remaining salamanders (MP bootstrap = 80%); in the MP tree inferred from the large dataset, *Proteus* and *Amphiuma* are a clade (MP bootstrap = 76%) and this clade plus Salamandridae is the sister taxon to a group containing all remaining salamanders (MP bootstrap = 90%). Because the parsimony method is known to show poor performance in handling highly heterogenous data, the results from parsimony analyses are thus not considered further.

Our topological test results are summarized in Table 4. These topological tests are specially designed to test the monophyly of the internally fertilizing salamanders (Salamandroidea), the monophyly of Proteidae, the position of Sirenidae, and the position of Proteidae. The monophyly of Salamandroidea is strongly supported by both DNA and protein data (opposite hypothesis always rejected; Table 4). The monophyly of Proteidae is somewhat unclear since its opposite hypothesis is rejected by the protein data but not the DNA data. The two alternative hypotheses for the placement of sirenids within salamanders are basically rejected by both the protein and DNA data, except that the hypothesis that Cryptobranchoidea is the sister group of other salamanders cannot be

Table 4
Statistical confidence (*P*-values) for alternative branching hypotheses of the ten living salamander families.

Data set	Alternative topology tested	Δln *L*	*P*-value		Rejection
			AU test	KH test	
Mitochondrial proteins	Best ML	0	0.993	0.954	– –
	Without monophyletic Salamandroidea	−49.6	0.012	0.012	+ +
	Without monophyletic Proteidae	−22.1	0.037	0.028	+ +
	Cryptobranchoidea branched earlier	−18.2	0.098	0.051	– –
	Sirenidae is sister to Cryptobranchoidea	−21.0	0.028	0.026	+ +
	Sirenidae is sister to Proteidae	−38.5	0.037	0.026	+ +
	Proteidae is sister to Ambys + Dicamp + Salam	−17.4	0.048	0.046	+ +
	Proteidae is sister to other Salamandroids	−17.5	0.053	0.044	– +
Mitochondrial DNA 3rd codon positions excluded	Best ML	0	0.975	0.895	– –
	Without monophyletic Salamandroidea	−41.6	0.045	0.043	+ +
	Without monophyletic Proteidae	−10.7	0.146	0.105	– –
	Cryptobranchoidea branched earlier	−27.0	0.011	0.010	+ +
	Sirenidae is sister to Cryptobranchoidea	−21.0	0.063	0.048	– +
	Sirenidae is sister to Proteidae	−79.4	0.001	<0.001	+ +
	Proteidae is sister to Ambys + Dicamp + Salam	−27.2	0.008	0.012	+ +
	Proteidae is sister to other Salamandroids	−28.2	0.003	0.009	+ +

rejected by the protein data, although the P values are close to the threshold of 0.05 (0.098 and 0.051; Table 4). These results suggest that Sirenidae is most likely the sister group to all other salamanders. The two alternative hypotheses for the placement of Proteidae within Salamandroidea are all rejected by both the protein and DNA data, by at least one of the tests used (Table 4). These results are strong evidence that Proteidae is the sister group to the Rhyacotritonidae–Amphiumidae–Plethodontidae clade.

Combining the phylogenetic results from both the protein and DNA data and the topological test results, we prefer the tree presented in Fig. 3. This tree will be used as the reference topology for molecular dating analyses (see below).

3.3. Molecular dating

Bayesian dating methods allow comparison of results from prior (fossil constraints) and posterior distribution analyses to examine how prior specifications affect the final posterior distribution results. The prior distribution analysis ignores the information contained in the sequence data; hence, it is expected that there will be a larger amount of uncertainty in prior divergence time estimates (Thorne and Kishino, 2002). Accordingly, we approximated the prior and posterior distribution of divergence times in both the Multidivtime and BEAST Bayesian dating analyses. The size of the 95% CI of the prior distribution for node ages is considerably larger than the size of the 95% CI of the posterior distribution and the means are also different in most cases (Table 5 and Table 6). These differences in means and the size of credibility intervals between the prior and posterior distribution indicate that the prior specification has little influence on the posterior distribution and that most of the information about divergence time is retrieved from the sequence data.

In the Multidivtime analyses, when not using the two internal maximal bounds suggested by Marjanović and Laurin (2007) (Table 5; 15C), the mean and 95% confidence interval for the origin of lissamphibians (327, 313–339 MYA) and for the Anura–Caudata

Table 5
Detailed results of Bayesian molecular dating using Multidivtime. Letters for nodes are corresponding to Fig. 4. 15C and 17C refer to using 15 or 17 fossil constraints (see Section 2), respectively.

Nodes	MultiDivTime Bayesian (95% C.I.) (MYA)			
	15C-Prior	15C-Posterior	17C-Prior	17C-Posterior
Lungfish–Tetrapod split (Ingroup root)*	413 (408–419)	411 (408–417)	413 (408–419)	411 (408–417)
Bird–Lizard split*	276 (253–299)	292 (280–300)	276 (253–299)	290 (276–299)
Bird–Crocodile split*	243 (235–251)	246 (237–251)	243 (235–251)	245 (237–251)
Alligator–Caiman split*	70 (66–75)	68 (66–72)	70 (66–75)	68 (66–72)
A: Amphibia–Amniote split*	348 (332–360)	357 (349–360)	346 (331–359)	352 (341–360)
B: Origin of living amphibians	328 (280–356)	327 (313–339)	305 (261–350)	308 (296–320)
C: Anura–Caudata split*	306 (257–348)	301 (285–316)	262 (251–274)	270 (261–275)
D: Origin of living salamanders*	281 (213–335)	210 (192–230)	165 (154–170)	169 (166–170)
E: Cryptobranchoidea–Salamandroidea split	255 (182–320)	192 (175–211)	159 (148–168)	161 (156–167)
F: Origin of Salamandroidea	226 (147–301)	180 (163–199)	143 (106–164)	149 (142–157)
G: Cryptobrachidae–Hynobiidae Split*	216 (150–295)	162 (147–182)	152 (145–164)	146 (145–150)
H: Origin of Hynobiidae	162 (59–263)	120 (105–138)	114 (45–155)	106 (97–115)
I: Dicamptodontidae–Ambystomatidae split*	133 (60–234)	132 (116–151)	91 (58–139)	110 (99–120)
J: Ambystomatidae–Salamandridae split	184 (94–273)	168 (151–187)	119 (73–155)	139 (131–147)
K: Origin of Salamandridae	138 (45–238)	117 (102–134)	89 (31–141)	97 (87–106)
L: Origin of Plethodontidae	97 (24–190)	109 (95–125)	62 (18–115)	90 (81–99)
M: Amphiumidae–Plethodontidae split	131 (48–226)	144 (128–162)	83 (33–132)	120 (110–129)
N: Rhyacotritonidae–Amphiumidae split	164 (76–255)	155 (138–173)	104 (54–146)	128 (119–137)
O: Proteidae–Rhyacotritonidae split	197 (112–280)	171 (154–190)	125 (82–156)	142 (134–150)
P: Proteus–Necturus split*	126 (59–228)	154 (136–173)	90 (57–139)	127 (117–137)
Q: Siren–Pseudobranchus split	136 (56–292)	85 (70–102)	81 (43–161)	66 (56–76)
R: Cryptobranchus–Andrias split	109 (53–239)	57 (47–69)	77 (39–149)	52 (44–60)

* Calibration points.

Table 6
Detailed results of Bayesian molecular dating using BEAST. Letters for nodes are corresponding to Fig. 4. 15C and 17C refer to using 15 or 17 fossil constraints (see Section 2), respectively.

Nodes	15C-Uniform		15C-Lognormal		17C-Uniform		17C-Lognormal	
	Prior	Posterior	Prior	Posterior	Prior	Posterior	Prior	Posterior
Lungfish–Tetrapod split (Ingroup root)*	413 (408–418)	413 (408–418)	415 (410–421)	415 (410–421)	413 (408–418)	413 (408–418)	415 (410–421)	415 (410–420)
Bird–Lizard split*	275 (252–297)	286 (270–300)	282 (262–308)	287 (270–309)	274 (252–297)	285 (268–300)	282 (262–307)	287 (269–308)
Bird–Crocodile split*	243 (235–250)	243 (236–251)	245 (238–254)	245 (238–254)	243 (235–250)	243 (235–250)	245 (238–254)	245 (238–253)
Alligator–Caiman split*	70 (66–75)	71 (67–75)	72 (68–77)	72 (68–73)	70 (66–75)	71 (67–75)	72 (68–77)	72 (68–78)
A: Amphibia–Amniote split*	345 (333–360)	345 (330–358)	352 (337–371)	349 (337–364)	345 (332–360)	342 (330–357)	350 (337–367)	348 (337–361)
B: Origin of living amphibians	321 (278–351)	300 (271–329)	325 (276–364)	302 (272–332)	300 (257–345)	290 (266–316)	304 (263–348)	294 (271–319)
C: Anura–Caudata split*	297 (250–336)	272 (250–298)	300 (250–341)	275 (250–304)	261 (250–273)	261 (250–273)	265 (255–278)	264 (255–276)
D: Origin of living salamanders*	271 (212–329)	213 (183–243)	274 (212–334)	214 (184–246)	165 (156–170)	168 (165–170)	169 (156–186)	183 (167–201)
E: Cryptobranchoidea–Salamandroidea split	247 (184–310)	193 (166–221)	250 (184–314)	194 (167–222)	159 (149–169)	160 (156–164)	163 (148–180)	171 (158–186)
F: Origin of Salamandroidea	220 (150–290)	179 (154–208)	221 (150–293)	181 (154–209)	145 (119–166)	149 (139–157)	148 (117–176)	160 (144–177)
G: Cryptobrachidae–Hynobiidae Split*	200 (145–264)	161 (145–184)	201 (145–267)	161 (145–185)	152 (145–162)	147 (145–150)	154 (145–168)	151 (145–162)
H: Origin of Hynobiidae	128 (30–221)	107 (73–144)	129 (32–225)	109 (75–146)	99 (35–155)	93 (62–124)	101 (33–156)	100 (70–130)
I: Dicamptodontidae–Ambystomatidae split*	115 (56–191)	114 (71–152)	116 (56–193)	118 (77–157)	89 (56–129)	96 (69–124)	90 (56–132)	106 (74–137)
J: Ambystomatidae–Salamandridae split	176 (94–256)	162 (134–192)	177 (95–256)	163 (135–193)	121 (81–158)	135 (120–148)	124 (80–162)	145 (125–165)
K: Origin of Salamandridae	125 (42–215)	104 (75–137)	126 (42–216)	103 (73–139)	89 (36–141)	90 (67–113)	90 (35–144)	96 (72–124)
L: Origin of Plethodontidae	80 (19–151)	109 (85–133)	81 (19–152)	109 (85–134)	58 (16–104)	89 (74–104)	59 (15–104)	98 (80–115)
M: Amphiumidae–Plethodontidae split	108 (35–186)	139 (113–166)	109 (35–187)	140 (112–166)	77 (30–125)	115 (101–130)	78 (30–128)	124 (107–143)
N: Rhyacotritonidae–Amphiumidae split	141 (60–223)	152 (126–179)	142 (62–227)	152 (124–179)	99 (51–144)	126 (113–139)	100 (50–147)	136 (118–153)
O: Proteidae–Rhyacotritonidae split	180 (102–259)	168 (143–197)	182 (101–261)	170 (143–198)	124 (86–159)	140 (128–151)	126 (83–162)	151 (134–168)
P: Proteus–Necturus split*	110 (56–187)	145 (113–179)	110 (56–188)	146 (112–179)	87 (56–128)	120 (96–139)	88 (56–131)	129 (103–153)
Q: Siren–Pseudobranchus split	98 (0–240)	73 (36–124)	99 (0–242)	74 (34–120)	66 (0–149)	61 (29–96)	67 (0–153)	66 (34–107)
R: Cryptobranchus–Andrias split	79 (0–185)	64 (35–103)	80 (0–187)	66 (36–102)	62 (0–138)	60 (32–95)	63 (0–140)	63 (35–94)

* Calibration points.

split (301, 285–316 MYA) are close to those published in our previous paper (337, 321–353 MYA; 308, 289–328 MYA; Zhang et al., 2005). When the two internal maximal bounds were used (Table 5; 17C), Multidivtime gave date estimates 20–30 MYA younger for most nodes than those from the 15C-analysis. In the BEAST analyses, when not using the two internal maximal bounds (Table 6; 15C), two calibration strategies using different parametric distributions (uniform and lognormal) produced similar mean and confidence intervals for each node. However, when using the two internal maximal bounds (Table 6; 17C), the "soft" bound strategy always gave date estimates about 10 MYA older than the "hard" bound strategy. This result shows that while the two maximal bounds suggested by Marjanović and Laurin (2007) are somewhat incongruent with the mitogenome DNA data, the "soft" bound strategy we used served to balance the conflict to some extent. In general, the mean for a certain node age calculated by BEAST is younger than that from Multidivtime; the confidence interval calculated by BEAST is wider than that from Multidivtime.

BEAST can estimate a parameter called "covariance" which indicates how much the evolutionary rate of a child branch is related to its parent branch's rate (rate-autocorrelation). As a result, the covariance parameters estimated by different BEAST runs were around 0.13 (close to 0) and their 95% confident intervals span zero. This result indicates that there is no strong evidence supporting rate-autocorrelation in our mitogenome data, which implies that the results from Multidivtime (based on rate-autocorrelation assumption) may be somewhat biased. Therefore, we consider the dating results from BEAST to be more reliable. Because it is difficult to judge whether we should use two internal maximal bounds or not, our strategy is to use them, but with caution (applying the "soft bound" strategy in this case). Moreover, based on a recently described Early Permian stem batrachian fossil, *Gerobatrachus hottoni*, Anderson et al.(2008) inferred that the divergence between frogs and salamanders occurred 270–260 Ma, which is closest to the time estimate based on BEAST with 17 fossil constraints and the soft bound strategy (Table 6; Node C, 264 Ma, CI 255–276). Therefore, we regard the BEAST dating results using all 17 fossil constraints and the soft calibration strategy (Table 6, 17C-lognormal) as our preferred, primary hypothesis concerning molecular dating analyses.

An illustration of the timescale of lissamphibian evolution based on our final dating results is shown in Fig. 4. The origins for Lissamphibia and Batrachia took place in Early Permian (~294 MYA) and Late Permian (~264 MYA), respectively. Living salamanders originated in Early Jurassic (~183 MYA). We compared our newly obtained molecular estimates for three nodes of interest (Lissamphibia, Batrachia, and Caudata) with results from other studies (see Table 7 for details). In comparison with previous molecular results, our time estimates are much younger than most, but close to those from a recent analysis of a large fragment of nuclear RAG1 gene for a limited sample (Hugall et al., 2007). Among all available molecular estimates, our new results are most compatible with the estimates based on fossils (Marjanović and Laurin, 2007), although some incongruence remains.

3.4. Biogeographic inferences

The overall log-likelihood for our Lagrange analysis was −188.044 with the use of $\lambda_D = 0.007$ and $\lambda_E = 0.001$. The most probable ancestral area for each node is shown in Fig. 5.The most recent common ancestor of all living salamanders likely possessed a wide-spread Laurasian distribution but support is moderate (relative probability = 69%; Fig. 5). The common ancestor of sirenid salamanders was isolated in Eastern North America in the early history of salamander evolution (relative probability = 100%; Fig. 5). Subsequently, a vicariance event took place that separated two lineages of ancestral salamanders, giving rise to

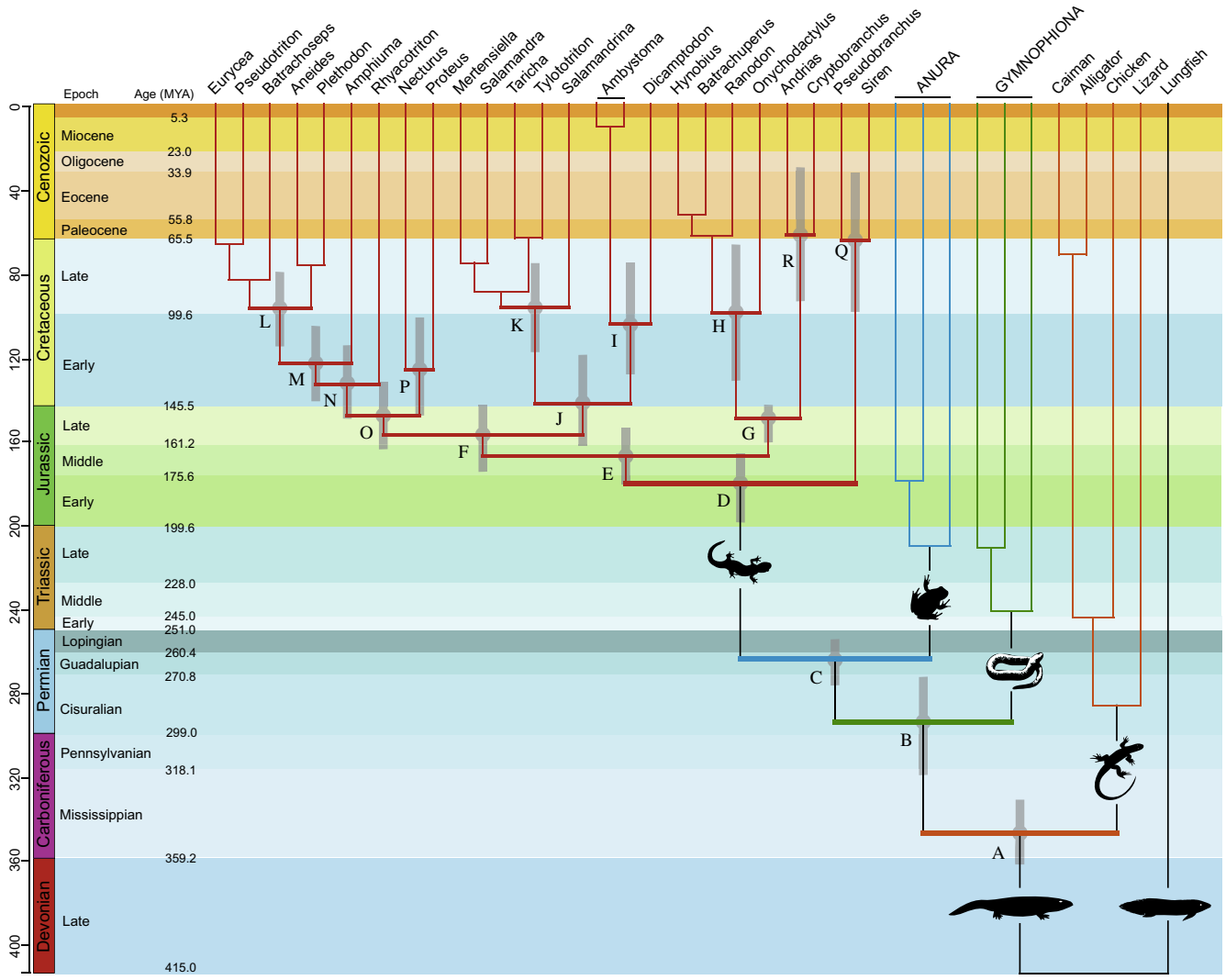

Fig. 4. Time-calibrated phylogeny of lissamphibians with an emphasis on living salamanders, fitted to a geological timescale. Times for nodes with letter labels beside them (also highlighted by thickened horizontal lines) are estimated by BEAST (soft-bound calibration strategy with 17 fossil constraints). The vertical gray bars through these nodes indicate 95% credibility intervals from the BEAST soft-bound analyses. For the sake of computational cost, our BEAST soft-bound analyses were only run for these nodes with letter labels. To make the time tree topology balanced, the times for other nodes (without letter labels and not highlighted by thickened horizontal lines) are represented according to time estimation means from the Multidivtime analyses (hard-bound calibration strategy with 17 fossil constraints). Detailed time estimates can be found in Table 4 and 5. An Early Permian origin for Lissamphibia and an Early Jurassic origin for salamanders are proposed.

Cryptobranchoidea in Eastern Eurasia (relative probability = 99%; Fig. 5) and Salamandroidea (internally fertilizing salamanders) in Euramerica (relative probability = 70%; Fig. 5). The site of origin for four Euramerican salamander families, the Amphiumidae, Plethodontidae, Proteidae, and Rhyacotritonidae, was likely Eastern North America (relative probability = 98%; Fig. 5).

4. Discussion

4.1. Is the rapidly evolving mitogenome suitable for deep phylogeny?

Mitochondrial DNA has been widely used in phylogenetic inference. The special features of mitochondrial DNA (i.e., lack of introns, maternal inheritance, absence of recombination, and haploidy) have made it the most common type of sequence information used to estimate phylogenies among both closely and distantly related taxa (Zardoya and Meyer, 1996). Moreover, because of the large quantity of data in mitogenomes, they have special value in estimation of timing of phylogenetic events. Nevertheless, in mammalian phylogenies, several early studies of mitochondrial genomes argued that Rodentia (the most speciose order of mammals) is paraphyletic (D'Erchia et al., 1996; Reyes et al., 1998; Reyes et al., 2000). These results challenge the monophyly of Rodentia, a group well-recognized on the basis of dentition, skull morphology, soft anatomy, the postcranial skeleton, and the jaw mechanism. The mitochondrial hypothesis was soon demonstrated to be problematic by more extensive studies employing primarily nuclear DNA sequences, which have resulted in higher levels of congruence with earlier morphological studies (Madsen et al., 2001; Murphy et al., 2001). This severe disagreement between nuclear DNA + morphology and mitochondrial DNA led to questions concerning the utility of mtDNA for studying deep phylogenies. Moreover, Springer et al.'s (2001) comparison of mitochondrial and nuclear gene sequences implied that mitochondrial data are less effective in resolving relationships at deeper nodes of the mammalian tree, and in many cases mitochondrial sequences will give "wrong answers". As a consequence, multiple nuclear genes have become favored for studies of deep phylogenies.

Initial diversification of living salamanders is thought, on the basis of fossils (Evans et al., 2005), to have taken place at least

Table 7
A comparison of time estimates on Lissamphibia evolution from different studies.

Study	Lissamphibia	Batrachia	Caudata	Method	Source of data	Calibration points and strategy
San Mauro et al. (2005)	367 (328–417)	357 (317–405)	273 (238–312)	MultiDivTime	1368 bp of RAG1	5 fossils, 4 geological events (hard bound)
Roelants et al. (2007)	369 (344–396)	358 (333–385)	249 (220–282)	MultiDivTime	3747 bp from 4 Nuclear + 1 mtDNA loci	15 fossils, 7 geological events (hard bound)
Roelants et al. (2007)	352 (304–370)	333 (289–353)	220 (196–247)	R8S; Penalized Likelihood	Same as above	Same as above
Hugall et al.(2007)	292 or 322	266 or 274	–	R8S; Penalized Likelihood	2613 bp of RAG1 or corresponding amino acids	1–5 calibration points (hard bound)
Zhang et al. (2005)	337 (321–353)	308 (289–328)	>197	MultiDivTime	7659 bp from mitogenome	2 from fossils (hard bound)
Marjanović and Laurin (2007)	260 (246–267)	254 (246–257)	162 (152–166)	Supertree	Fossils	–
This study	294 (271–319)	264 (255–276)	183 (167–201)	BEAST	9202 bp from mitogenome	17 from fossils (soft bound)

150 million years ago (Late Jurassic). Resolution of such a deep phylogeny by the rapidly evolving mitochondrial genome might be thought to be problematic because of the risk of saturation. Efforts to use mitochondrial fragments to estimate salamander phylogenetic relationships either resulted in poorly resolved phylogenies (Hedges and Maxson, 1993; Hay et al., 1995) or in phylogenies that were greatly incongruent with morphological studies (Weisrock et al., 2005). In contrast to these mitochondrial studies, application of nuclear gene sequences shows better performance in tree resolution and higher levels of congruence with earlier morphological studies, including high support for monophyly of a clade that includes all internally fertilizing salamanders (Wiens et al., 2005; Roelants et al., 2007). Moreover, Weisrock et al.'s simulation results (2005) suggest that the mtDNA data have limited ability to recover relatively old and short branches and may not provide substantial support for many branching events deep in salamander phylogeny. In contrast to the findings of Weisrock et al. (2005), our results show that mtDNA data are effective in resolving deep nodes within Caudata. Most of the nodes in our trees have bootstrap support levels of >90% and Bayesian posterior probabilities of >0.95, and the topology is largely congruent with those from morphological and nuclear data but better resolved. An intractable problem when using mtDNA to study deep phylogeny is the high rate heterogeneity among the data, which makes it difficult to infer a correct gene tree. Kjer and Honeycutt (2007) used a "site-specific" strategy to remodel mitochondrial genome data for mammals and recovered a phylogeny reasonably congruent with those derived from morphology and nuclear genes. The previous discordance between mitochondrial genomes and nuclear genes (and morphology) may be attributed largely to incomplete or inappropriate analyses of the mitochondrial genomes. In order to obtain correct gene trees when using rapidly evolving mitogenomes, it is critical to use appropriate analytical strategies. In this study, detecting and removing potentially saturated sites (3rd codon positions) to decrease the heterogeneity of mitogenome data, and using appropriate partition strategies to better describe substitution processes of mitogenome data, are good strategies and appear to work well. We believe that mitogenomic phylogenies will continue to provide important reference hypotheses for the continuing quest to recover the evolutionary history of organisms.

4.2. Is the family-level classification of salamanders appropriate?

There have now been sufficient studies of the ten commonly accepted salamander families to leave little doubt as to the validity of Amphiumidae, Ambystomatidae, Cryptobranchidae, Hynobiidae, Plethodontidae, Salamandridae, and Sirenidae as monophyletic (also recovered in this study). The genus *Rhyacotriton*, the sole member of the Rhyacotritonidae (formerly placed with *Dicamptodon* in the salamander family Dicamptodontidae) was raised to family level by Good and Wake (1992) to acknowledge its evolutionary distinctness. *Rhyacotriton* is only a distant relative to *Dicamptodon* in our trees (see also Larson and Dimmick, 1993; Weisrock et al., 2005; Wiens et al., 2005; Frost et al., 2006; Roelants et al., 2007), and we consider the recognition of this clade as a family appropriate. The genus *Dicamptodon*, formerly placed in the Ambystomatidae, was raised to family level, Dicamptodontidae, by Edwards (1976). Frost et al. (2006) returned *Dicamptodon* to the Ambystomatidae on the grounds that the two formed a clade and that each was monotypic. Given that *Dicamptodon* has a long fossil record dating to the Paleocene (Estes, 1981), that it differs from *Ambystoma* in easily visible features of morphology (Good and Wake, 1992), and in having perennial, stream-adapted larvae rather than generally short-lived (except for neotenic populations) pond larvae as in most *Ambystoma*, we believe there is reason to

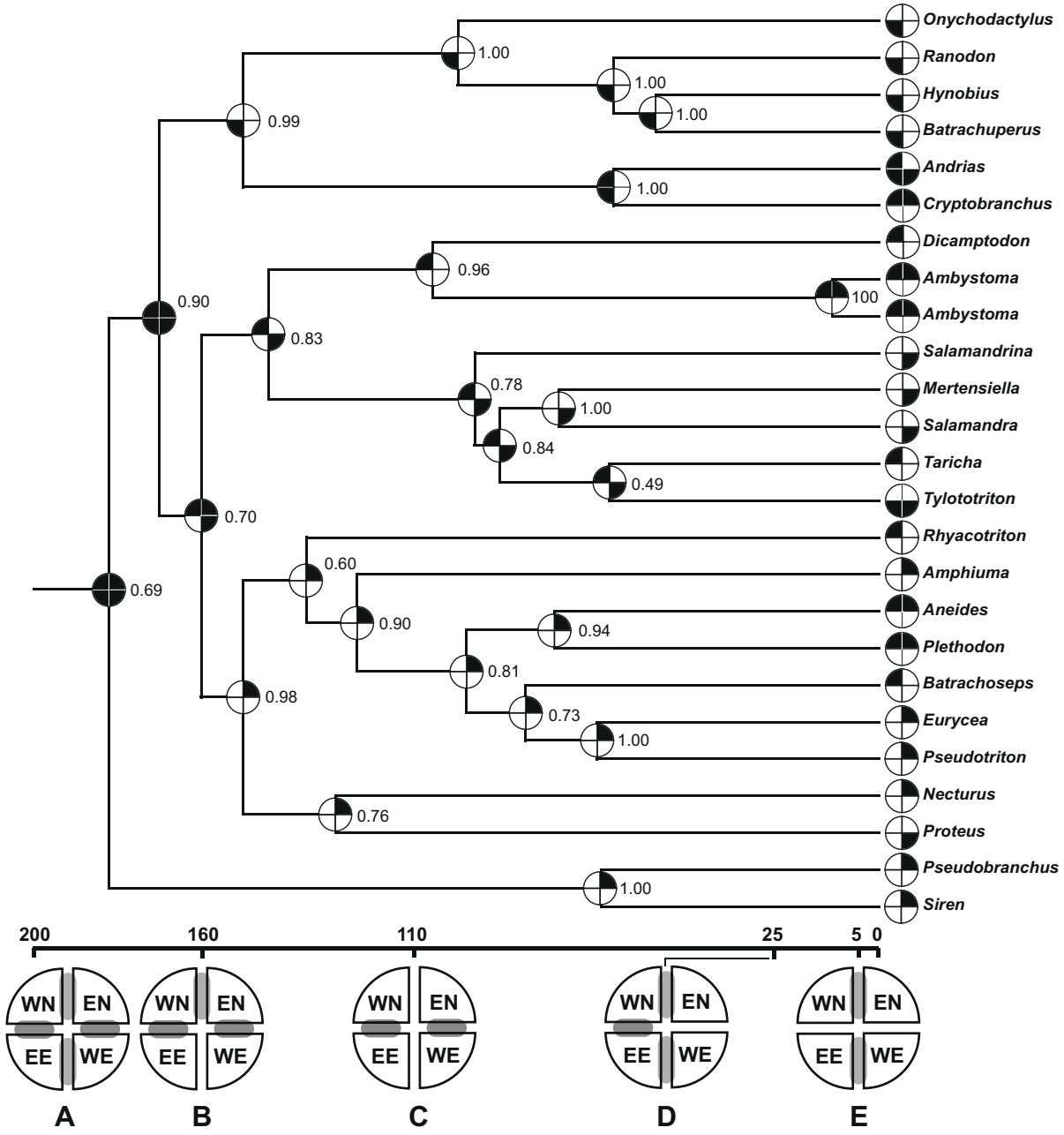

Fig. 5. Likelihood estimates of ancestral ranges for living salamanders using Lagrange program (Ree et al., 2005). The distribution of salamanders are divided into four areas: eastern North America (EN), western North America (WN), eastern Eurasia (EE), and western Eurasia (WE), represented as four different corners of a circle (see big circles under the timescale for details). Five major paleogeological events about the connections between areas are shown below the timescale as big circles: (A) uniform Landmass in Early Jurassic; (B) the formation of Turgai Sea in Mid Jurassic separated EE with WE; (C) epicontinental seaway in Cretaceous separated WN with EN. (D) the breakage of North Atlantic land bridge separated EN with WE; (E) the closure of Bering land bridge separated EE with WN. Only the biogeographic scenario with the highest likelihood is reported for each internal node. Numbers beside nodes are the probability of a reported biogeographic scenario relative to all possible scenarios for that node. A distribution throughout Laurasia in Early Jurassic for the common ancestor of all living salamanders is proposed.

continue to recognize Ambystomatidae and Dicamptodontidae as separate families.

The inclusion of the European *Proteus* and the North American *Necturus* in the family Proteidae has been contentious in the past, and the monophyly of this family has been questioned based on both morphological (Hecht and Edwards, 1976) and molecular (Weisrock et al., 2005) data. We find strong support for the monophyly of Proteidae (ML bootstrap >95%) (also found by others based either on relatively small datasets, Trontelj and Goricki, 2003, and Wiens et al., 2005, or with only moderate support, Roelants et al., 2007). However, in this study, the hypothesis of paraphyly of the family can only be rejected by the mitochondrial protein data, not by the DNA data (Table 4). Furthermore, the divergence between *Necturus* and *Proteus* is in our opinion sufficiently deep to warrant recognition of two families (Fig. 4), especially if we base our decision on the separation of Dicamptodontidae and Ambystomatidae as a paradigm. If a paraphyletic Proteidae is enforced, our further analyses (results not shown) indicate that the European *Proteus* is the sister group to a *Necturus* + Rhyacotritonidae + Amphiumidae + Plethdontidae clade (all New World in distribution except for a handful of deeply nested Old World plethodontids). This relationship would be interesting because we would have a European lineage sister to a North American one, which has apparent biogeographic implications. While the molecular data are

somewhat equivocal on the monophyly of Proteidae in the traditional sense, the fact that the two genera (*Proteus* and *Necturus*) share a unique chromosome number among salamanders (19 pairs; Morescalchi, 1975) may be a significant signal of monophyly. Therefore, we think maintaining the family status for Proteidae to include both *Proteus* and *Necturus* is justified. Resolution of this problem must await the collection of new data.

4.3. Mitogenomic perspectives on higher-level salamander relationships

Historically two hypotheses have been presented for the initial phylogenetic split within living salamanders. Either the Sirenidae, or the clade comprised of Cryptobranchidae + Hynobiidae (Cryptobranchoidea), diverged first. The characters that support a basal position of crypotobranchoids are the demonstrable external fertilization (considered plesiomorphic) of cryptobranchoids, their possession of a bone in the lower jaw (angular) that is characteristic of Paleozoic relatives but not found in other living salamanders, and higher chromosome numbers (with only one exception, *Hynobius retardatus*) than other salamanders, including many microchromosomes (Edwards, 1976). Sirenids are permanently larval species that offer a bizarre combination of traits (cornified beaks rather than teeth on the jaws, no hind limbs or girdles), and they are suspected to have external fertilization (Sever et al., 1996). They were even considered to belong to a fourth lissamphibian order, Trachystomata, by Goin et al. (1978).

Sirenidae is usually presented as the most basal of the extant salamander families (Duellman and Trueb, 1986). This hypothesis was supported by earlier molecular studies (Larson and Dimmick, 1993; Hedges and Maxson, 1993; Hay et al., 1995) but these studies were deficient in relevant data and contained neither convincing statistical support nor topological tests. Recent studies have continued to find sirenids nested within the salamander phylogeny but some problems still remain. Gao and Shubin (2001) found sirenids to be close relatives of proteids in their reassessment of nuclear RNA and morphological data, but they did not perform statistical tests for branch support. Frost et al. (2006) found the same result but questions have been raised concerning their data quality control and analytical methods (Wiens, 2007). Wiens et al. (2005) found sirenids to be sister to the internally fertilizing salamanders based on combined molecular and morphological data, but they did not perform a bootstrapping test. Roelants et al. (2007) have the most comprehensive molecular dataset published to date, and they supported the hypothesis that sirenids are sister group to Salamandroidea, but they have only modest support (ML bootstrap = 62%) for that node.

Our analyses of mitochondrial genomes favor the hypothesis that Sirenidae is the sister-taxon to other living salamanders. The corresponding node is strongly supported for both the protein and the DNA analyses (protein ML bootstrap = 96%, DNA ML bootstrap = 98%). Moreover, the topological tests comparing the three possible relationships among Sirenidae, Cryptobranchoidea, and Salamandroidea indicate that the hypothesis of Sirenidae as the basal branch is significantly stronger than the hypothesis of Cryptobranchoidea as the basal branch (Table 4, $P < 0.05$). We cannot reject a monophyletic origin for salamanders thought to be externally fertilizing (Sirenidae and Cryptobranchoidea) (Table 4, $P_{AU} = 0.063$), a hypothesis that has never been proposed to our knowledge.

A basal position for Sirenidae would make interpretation of some of its traits more intuitive. For example, sirenids lack all cloacal glands (Sever et al., 1996) normally associated with spermatophore production and internal fertilization in crown-group salamanders, while cryptobranchoids have one of the three kinds of glands. The sperm of sirenids have two flagella, a situation also found in basal frog lineages (frogs are the closest relatives of salamanders), while the sperm of other salamanders (including cryptobranchoids) only has a single flagellum (Scheltinga and Jamieson, 2003). Sirenids have a primitive pectoral girdle similar to that of frogs in having the scapula and coracoid present as separate bones, while the scapula and coracoid are fused to form a combined scapulocoracoid in other salamanders. The nasal bones of sirenids are thought to be derived from lateral nasals only, whereas those of other salamanders appear to represent both lateral and medial nasals (Good and Wake, 1992). Nevertheless, given that the mitochondrial genome is a single locus, one must exercise caution not to over-interpret our result. The discordance between our mitogenomic result and the results from nuclear data (e.g. Roelants et al., 2007) leaves the placement of Sirenidae tentative for now. Because the number of nuclear loci currently used to infer the phylogeny of salamanders is low (no more than four), no strong consensus has been attained.

The internally fertilizing salamanders of the clade Salamandroidea (all salamanders except Sirenidae, Cryptobranchidae, and Hynobiidae) are usually thought to be monophyletic. This clade is well supported by morphological and life-history characters. Nevertheless, analyses of nuRNA and morphology (Gao and Shubin, 2001) and nuclear and mitochondrial DNA sequences (Frost et al., 2006) found Sirenidae (which most likely practices external fertilization) to be the sister-taxon of Proteidae, which would question the monophyly of the Salamandroidea. Hecht and Edwards (1981) argued "once a group has achieved internal fertilization by means of a spermatophore, it does not seem likely to us that this very specialized means of inserting the sperm into the female would have been abandoned for a presumably much more hazardous method (external fertilization)." Monophyly of the internally fertilizing salamanders is strongly supported in the current study (DNA ML bootstrap = 98%, protein ML bootstrap = 91%), as found also in other studies but with lower support (Larson and Dimmick, 1993; Wiens et al., 2005; Roelants et al., 2007). The hypothesis of non-monophyly for Salamandroidea can also be rejected statistically (Table 4, $P < 0.05$). These results suggest that the grouping of Proteidae and Sirenidae recovered by other authors (Gao and Shubin, 2001; Frost et al., 2006) is problematic, probably for the following reasons: paedomorphic evolution of characters, inadequate taxon sampling, and poor performance of molecular data.

Relationships within the Salamandroidea from this study are basically concordant with most published hypotheses. The only remaining uncertainty concerning relationships is the exact placement of Proteidae (including *Necturus*). Morphologically, Proteidae is thought to be the basal lineage within Salamandroidea (Duellman and Trueb, 1986) but this hypothesis has not been tested statistically. Proteidae has been recovered as the sister-taxon to a clade including Salamandridae, Dicamptodontidae, and Ambystomatidae (Hedges and Maxson, 1993; Larson and Dimmick, 1993; Wiens et al., 2005), but with either weak (bootstrap <50%) or moderate (bootstrap <70%) support. Roelants et al. (2007) analyzed a large dataset combining four nuclear loci and one mitochondrial fragment (~4200 bp) and favored Proteidae as the sister-group to a clade including Plethodontidae, Amphiumidae, and Rhyacotritonidae (ML bootstrap >75%). We recovered the same topology, with stronger support (ML bootstrap > 98%). Our topological tests further indicate that the hypothesis of (Proteidae, (Rhyacotritonidae, (Plethodontidae, Amphiumidae))) is statistically stronger than both the hypothesis (Proteidae, (Salamandridae, (Dicamptodontidae, Amystomatidae))) and the hypothesis that Proteidae is a distant sister taxon to all other internally fertilizing salamanders (Table 4).

4.4. Timescale for modern salamanders and historical biogeography

Based on fossils, salamanders have been present in modern form at least since mid-Jurassic times (>150 MYA), and both extant

and fossil taxa have a nearly exclusive Laurasian distribution. All salamander lineages arose in the Laurasian part of Pangea and are thought to have undergone diversification concomitant to the continental breakups (Milner, 1983; Duellman and Trueb, 1986). Based on nuclear gene data and Bayesian dating methods, some studies give a late Paleozoic origin (273, 238–312 MYA; San Mauro et al., 2005) or an early Mesozoic origin (249, 220–282 MYA; Roelants et al., 2007) for salamanders, much older than expected from inference based on the fossil record (152–166 MYA; Marjanović and Laurin, 2007). Our estimates of divergence times suggest that the common ancestors of modern salamanders occurred in the Early Jurassic, around 183 MYA, which is younger than all available molecular estimates, but still somewhat older than dates inferred from fossils (summarized by Vieites et al., 2009). Mesozoic sirenid (basal branch in our phylogeny) fossils from both South America (*Noterpeton*) and Africa (*Kababisha*) (Evans et al. 1996) can be offered as qualified evidence that the initial diversification of salamanders predated the breakup of Pangea in the Mid-Early Jurassic (160–200 MYA). However, the nearly exclusive Laurasian distribution for extant and fossil salamanders implies that the origin of salamanders is unlikely to have happened much earlier than the breakup of Pangea; consequently, an Early Jurassic origin for salamanders seems logical. Regarding the early branches of the salamander lineage, Cryptobranchoidea has a mainly Asian distribution and Sirenidae has a North American distribution (although fossils thought to be sirenids penetrated into South America and Africa). Salamandroidea possess a fundamentally Holarctic distribution centered in North America and Europe. Any hypotheses concerned with the place of origin for salamanders depend largely on the relationships among these three major clades. If it is Cryptobranchoidea that branched earliest, as suggested by current nuclear data (Wiens et al., 2005; Roelants et al., 2007), the most parsimonious biogeographic scenario for the early evolution of salamanders would be as follows: the stem of Caudata possessed a Laurasian distribution and then was divided into two groups by a vicariance event between Asia and Euramerica, providing the ancestral stock of cryptobranchoids in Asia and of sirenids + salamandroids in Euramerica. On the other hand, based on our phylogenetic hypothesis, which favors Sirenidae as the basal branch, our ancestral area reconstruction analyses still indicate that the common ancestor of all living salamanders was distributed throughout the whole Laurasia landmass in the Early Jurassic (Fig. 5), suggesting that the biogeographic inference for the origin place of salamanders will not change no matter which salamander major relationships we use.

Our data suggest that sirenid salamanders diverged from other salamanders in the Early Jurassic (~183 MYA), a time when the North Atlantic Ocean began to open (Hallam, 1994). The opening of the North Atlantic Ocean started along the eastern margins of North America and South America-Africa first, which is congruent with the distribution of extant and fossil sirenids. If our salamander phylogeny and divergence time estimates are correct, the ancestral sirenids may have been restricted to small land margins along eastern North America-South America-Africa while the North Atlantic Ocean opened. The second divergence event that gave rise to Cryptobranchoidea in Asia and Salamandroidea in Euramerica took place in the Mid-Jurassic (~171 MYA), according to our salamander timetree (Fig. 4). Geologically, the Turgai Sea formed in the Mid-Jurassic (~160 MYA), separating eastern Asia from Europe and North America (Briggs, 1995). Although the two times are 10 million years different, their geological periods are identical, implying that the formation of the Turgai Sea may be the geological driving factor for the Cryptobranchoidea–Salamandroidea split. Duellman and Trueb (1986) proposed a North American origin for Cryptobranchoidea. However, our data strongly support an eastern Eurasian origin in Late Jurassic for this clade (likelihood percent = 99%; Fig. 5). This result is consistent with many fossil findings of cryptobranchoid or cryptobranchoid-related salamanders from Jurassic–Cretaceous deposits in the northern China (Gao and Shubin, 2001, 2003; Wang, 2004). The North American cryptobranchids (*Cryptobranchus*) may be a result of later dispersal from Asia, probably eastward through a Bering land bridge because the westward way was blocked by the Turgai Sea during that time. The common ancestor of all internally fertilizing salamanders (Salamandroidea) possessed a Euramerican distribution in the Mid-Jurassic (~160 MYA; likelihood percent = 70%; Fig. 5). This finding is at odds with the inference from fossil records that Salamandroidea originated around 80 million years ago (Marjanović and Laurin, 2007). Salamandroid-related fossils are known from Mid-Jurassic (vertebrae fragments; Evans and Waldman, 1996) to Late Jurassic (*Iridotriton*; Evans et al., 2005), which is fairly close to our time estimate. The fossil inference depends largely on the phylogenetic relationships among extant and fossil taxa, different topologies leading to different answers, and thus such discordance is understandable.

Plethodontidae, Salamandridae and Hynobiidae, the three most speciose salamander families containing nearly 90% of extant salamander species, are mostly distributed in America, Europe and Asia, respectively. Initial diversification of these three clades occurred at nearly the same period, ca. 96–100 million years ago (nodes L, K & H; Table 6 and Fig. 4), implying that there may have been a global event acting as the major factor in their diversification. This pattern is similar to those reported in such other taxa as birds, mammals, ants and angiosperms (Ericson et al., 2006; Moreau et al., 2006; Bininda-Emonds et al., 2007), with a radiation of major clades around the beginning of Late Cretaceous (~100 MYA). The Late Cretaceous experienced a global warming event, with significantly higher temperatures in northern latitudes (Zachos et al., 2001; Jenkyns et al., 2004). It is well known that most salamanders are adapted to low temperatures. The global warming in the Late Cretaceous might have driven many salamander taxa to extinction, causing a previously continuous fauna to split into many geographically isolated groups, and perhaps stimulating the diversification of plethodontids in America, salamandrids in Europe and hynobiids in Asia. Furthermore, subsequent dispersal of salamandrids and plethodontids between continents would have been facilitated by the shorter distances at high latitudes and the availability of newly opening niches in the north while the global warming progressed (Vieites et al., 2007; Zhang et al., 2008).

4.5. Dating incongruence for lissamphibian evolution

Building the early evolutionary history of lissamphibians is an active area of research at present. The earliest lissamphibian fossils, *Triadobatrachus* and *Czatkobatrachus*, are found in Early Triassic deposits of ~250 MYA. However, recent efforts to date the time of initial diversification of lissamphibians using molecular data suggest that lineages were established far earlier, perhaps as far back as the Permian period about 294 MYA (Hugall et al., 2007; this study), the Carboniferous period about 337 MYA (Zhang et al., 2005), or even the latest Devonian period about 367 MYA (San Mauro et al., 2005; Roelants et al., 2007). Marjanović and Laurin (2007) compiled a supertree including 223 extinct species of lissamphibians and gave a statistical evaluation of fossils that bear on this question. They proposed that Lissamphibia arose some 260 million years ago, much younger than the current molecular calculations.

The comparison of time estimates of lissamphibian evolution from different studies (Table 7) suggests that the methods used is influential; dates from Multidivtime (Thorne and Kishino, 2002) are systematically older than those from R8S (Sanderson,

2003). Such differences in time estimation may be attributed to features of the two methods. Multidivtime accommodates unlinked rate variation across different loci (a 'multigene' approach), but uses a rather simple F84 + G model for branch length estimation. R8S's penalized likelihood method needs a third-party software for branch length estimation, allowing the use of more complex DNA substitution models (e.g., GTR + I + Γ), but necessarily averages rate variation over all loci (a 'supergene' approach). Technically, both of the above two methods are based on a rate-autocorrelation assumption (child branch rates tend to relate to parent branch rates); they both try to depress the rate change across branches. Because it is unknown how variable the rate change throughout the amphibian phylogeny will be (obviously it is highly variable), applying the assumption of rate autocorrelation is risky because rate change across the phylogeny is restricted within a smaller range, which will in turn result in biased estimates and inauthentic shorter confident intervals. The program BEAST (Drummond et al., 2006) may be more realistic: it accommodates a rate-uncorrelated framework and can analyze multiple loci or site partitions simultaneously while accounting for their differences in evolutionary dynamics, also allowing the use of different DNA substitution models, including self-created ones. However, Rannala and Yang (2007) pointed out that BEAST's rate-uncorrelated implementation introduces negative correlation into the prior between branch rates so that the model tends to underestimate possible positive autocorrelations in rates across branches, although they also indicated that the effect should become minor in large trees with many branches, which is normally the case for real data. In any case, each method will ineluctably have both advantages and limitations, thus leaving the choice of program for lissamphibian molecular dating an open question.

Another important reason for discordances among studies of lissamphibian evolution is the choice of fossil calibrations and calibration strategies. The current trend of applying most fossil constraints as minima with a maximum root constraint appears logical because fossils often provide good minimal bounds, but not maximal bounds. However, this strategy leads to a consistent bias towards inflating dating estimates, as indicated by Yang and Rannala (2006). In such analyses, a single calibration point with a maximal bound can largely scale the tree (and all other calibrations will have little effect), and model fitting artifacts can further increase basal branch lengths until the maximum age constraint is reached, which makes the dates for each node a maximum possible age (Hugall et al., 2007). Therefore, more calibration points with maximal bounds are needed to depress such an inflation artifact, which is also the main point suggested by some paleontologists (Marjanović and Laurin, 2007). However, in the case of the Lissamphibia, for which the fossil record is not good, we face a potential risk: imposing too many uncorroborated maximal bounds can constrain the result to say nothing more than what the fossils present, obscuring information in the molecular data. Using a "soft bound" calibration strategy as we did in this study is an attempt to depress the inflating artifact of molecular dating while letting the molecular data speak for themselves. The method that should be used to describe a "soft bound" constraint is still a subjective issue and deserves further discussion elsewhere.

Acknowledgments

R. Bonett and the MVZ Herpetology Collection provided tissue samples. We thank J. McGuire for assistance with parallel computing and the MVZ Cluster for providing computer resources. D. Buckley, A. Leaché, D. Vieites, J. McGuire, K. Whittaker, M. Laurin and T. Papenfuss provided helpful comments on earlier drafts of this manuscript. M. Wake discussed the work with us and provided a careful review of the manuscript. Special thanks go to D. Marjanović for insightful suggestions that improved our data analyses, and to D. Buckley for helping to implement BEAST. R. Ree offered assistance in interpretation of the results of the Lagrange program. This work was supported by the AmphibiaTree Project (NSF EF-0334939).

References

AmphibiaWeb: Information on amphibian biology and conservation [web application]. Berkeley, California: AmphibiaWeb. Available from: http://amphibiaweb.org/ (Accessed: June, 2009).
Anderson, J.S., Reisz, R.R., Scott, D., Fröbisch, N.B., Sumida, S.S., 2008. A stem batrachian from the Early Permian of Texas and the origin of frogs and salamanders. Nature 453, 515–518.
Anisimova, M., Gascue, O., 2006. Approximate likelihood-ratio test for branches: A fast, accurate, and powerful alternative. Syst. Biol. 55, 539–552.
Arnason, U., Gullberg, A., Janke, A., Joss, J., Elmerot, C., 2004. Mitogenomic analyses of deep gnathostome divergences: a fish is a fish. Gene 333, 61–70.
Benton, M.J., Donoghue, P.C., 2007. Paleontological evidence to date the tree of life. Mol. Biol. Evol. 24, 26–53.
Bininda-Emonds, O.R., Cardillo, M., Jones, K.E., MacPhee, R.D., Beck, R.M., Grenyer, R., Price, S.A., Vos, R.A., Gittleman, J.L., Purvis, A., 2007. The delayed rise of present-day mammals. Nature 446, 507–512.
Briggs, J.C., 1995. Global Biogeography. Elsevier Science, Amsterdam.
Brochu, C.A., 2004. Patterns of calibration age sensitivity with quartet dating methods. J. Paleont. 78, 7–30.
Castresana, J., 2000. Selection of conserved blocks from multiple alignments for their use in phylogenetic analysis. Mol. Biol. Evol. 17, 540–552.
D'Erchia, A.M., Gissi, C., Pesole, G., Saccone, C., Arnason, U., 1996. The guinea pig is not a rodent. Nature 381, 597–600.
Drummond, A.J., Ho, S.Y., Phillips, M.J., Rambaut, A., 2006. Relaxed phylogenetics and dating with confidence. PLoS Biol. 4, e88.
Duellman, W.E., Trueb, L., 1986. Biology of Amphibians. McGraw-Hill, New York.
Edwards, A.W.F., 1992. Likelihood. Johns Hopkins Univ. Press, Baltimore.
Edwards, J., 1976. Spinal nerves and their bearing on salamander phylogeny. J. Morphol. 148, 305–327.
Ericson, P.G., Anderson, C.L., Britton, T., Elzanowski, A., Johansson, U.S., Kallersjo, M., Ohlson, J.I., Parsons, T.J., Zuccon, D., Mayr, G., 2006. Diversification of Neoaves: integration of molecular sequence data and fossils. Biol. Lett. 2, 543–547.
Estes, R., 1981. Gymnophiona, Caudata. Handbuch der Palaoherpetologie 2, 1–115.
Evans, S.E., Milner, A.R., Werner, C., 1996. Sirenid salamanders and a gymnophionan amphibian from the Cretaceous of the Sudan. Palaeontology 39, 77–95.
Evans, S.E., Waldman, M., 1996. Small reptiles and amphibians from the Middle Jurassic of Skye, Scotland. Mus. Northern Arizona Bull. 60, 219–226.
Evans, S.E., Borsuk-Bialynicka, M., 1998. A stem-group frog from the Early Triassic of Poland. Acta Palaeontol. Polon. 43, 573–580.
Evans, S.E., Lally, C., Chure, D.C., Elder, A., Maisano, J.A., 2005. A Late Jurassic salamander (Amphibia: Caudata) from the Morrison Formation of North America. Zool. J. Lin. Soc. 143, 599–616.
Frost, D.R., Grant, T., Faivovich, J., Bain, R.H., Haas, A., Haddad, C.F.B., De Sa, R.O., Channing, A., Wilkinson, M., Donnellan, S.C., Raxworthy, C.J., Campbell, J.A., Blotto, B.L., Moler, P., Drewes, R.C., Nussbaum, R.A., Lynch, J.D., Green, D.M., Wheeler, W.C., 2006. The amphibian tree of life. Bull. Am. Mus. Nat. Hist. 297, 1–370.
Gao, K.Q., Shubin, N.H., 2001. Late Jurassic salamanders from northern China. Nature 410, 574–577.
Gao, K.Q., Shubin, N.H., 2003. Earliest known crown-group salamanders. Nature 422, 424–428.
Goin, C.J., Goin, O.B., Zug, G.R., 1978. Introduction to Herpetology. W.H. Freeman, San Francisco.
Good, D.A., Wake, D.B., 1992. Geographic variation and speciation in the torrent salamanders of the genus Rhyacotriton (Caudata: Rhyacotritonidae). Univ. Calif. Public. Zool. 126, 1–91.
Graur, D., Martin, W., 2004. Reading the entrails of chickens: molecular timescales of evolution and the illusion of precision. Trends Genet. 20, 80–86.
Guindon, S., Gascuel, O., 2003. A simple, fast, and accurate algorithm to estimate large phylogenies by maximum likelihood. Syst. Biol. 52, 696–704.
Gutell, R.R., Larsen, N., Woese, C.R., 1994. Lessons from an evolving rRNA: 16S and 23S rRNA structures from a comparative perspective. Microbiol. Rev. 58, 10–26.
Hallam, A., 1994. An Outline of Phanerozoic Biogeography. Oxford Univ. Press, Oxford.
Hay, J.M., Ruvinsky, I., Hedges, S.B., Maxson, L.R., 1995. Phylogenetic relationships of amphibian families inferred from DNA sequences of mitochondrial 12S and 16S ribosomal RNA genes. Mol. Biol. Evol. 12, 928–937.
Hecht, M.K., Edwards, J.L., 1976. The determination of parallel or monophyletic relationships: the proteid salamanders—a test case. Am. Nat. 110, 653–677.
Hecht, M.K., Edwards, J.L., 1981. The methodology of phylogenetic inference above the species level. In: Hecht, M.K., Goody, P.C., Hecht, B.M. (Eds.), Major Patterns in Vertebrate Evolution. Plenum Press, New York, pp. 3–51.
Hedges, S.B., Maxson, L.R., 1993. A molecular perspective on lissamphibian phylogeny. Herpetol. Monogr. 7, 27–42.
Huelsenbeck, J.P., Ronquist, F., 2001. MRBAYES: Bayesian inference of phylogenetic trees. Bioinformatics 17, 754–755.

Hugall, A.F., Foster, R., Lee, M.S.Y., 2007. Calibration choice, rate smoothing, and the pattern of tetrapod diversification according to the long nuclear gene RAG-1. Syst. Biol. 56, 543–563.
Jenkyns, H.C., Forster, A., Schouten, S., Sinninghe Damste, J.S., 2004. High temperatures in the Late Cretaceous Arctic Ocean. Nature 432, 888–892.
Kishino, H., Hasegawa, M., 1989. Evaluation of the maximum likelihood estimate of the evolutionary tree topologies from DNA sequence data, and the branching order in Hominoidea. J. Mol. Evol. 29, 170–179.
Kjer, K.M., 1995. Use of rRNA secondary structure in phylogenetic studies to identify homologous positions: an example of alignment and data presentation from the frogs. Mol. Phylogenet. Evol. 4, 314–330.
Kjer, K.M., Honeycutt, R.L., 2007. Site specific rates of mitochondrial genomes and the phylogeny of eutheria. BMC Evol. Biol. 7, 8.
Larson, A., Dimmick, W.W., 1993. Phylogenetic relationships of the salamander families: an analysis of congruence among morphological and molecular characters. Herpetol. Monogr. 7, 77–93.
Larson, A., Weisrock, D.W., Kozak, K.H., 2003. Phylogenetic systematics of salamanders (Amphibia: Urodela), a review. In: Sever, D.M. (Ed.), Reproductive Biology and Phylogeny of Urodela (Amphibia). NH Science Publishers, Enfield, pp. 31–108.
Madsen, O., Scally, M., Douady, C.J., Kao, D.J., DeBry, R.W., Adkins, R., Amrine, H.M., Stanhope, M.J., de Jong, W.W., Springer, M.S., 2001. Parallel adaptive radiations in two major clades of placental mammals. Nature 409, 610–614.
Manchester, S.R., 1999. Biogeographical relationships of North American Tertiary floras. Ann. Mo. Bot. Gard. 86, 472–522.
Marjanović, D., Laurin, M., 2007. Fossils, molecules, divergence times, and the origin of lissamphibians. Syst. Biol. 56, 369–388.
Milner, A.R., 1983. The biogeography of salamanders in the Mesozoic and early Cenozoic: a cladistic vicariance model. In: Sims, R.W., Price, J.H., Whalley, P.E.S. (Eds.), Evolution, Time, and Space. The Emergence of the Biosphere. Academic Press, New York, pp. 431–468.
Milner, A.R., 1988. The relationships and origin of the living amphibians. In: Benton, M.J. (Ed.), The Phylogeny and Classification of the Tetrapods, vol. 1. Amphibians, Reptiles, Birds Systematics Association Special Volume 23. Academic Press, New York, pp. 59–102.
Milner, A.R., 2000. Mesozoic and tertiary Caudata and Albanerpetontidae. In: Heatwole, H., Carroll, R.L. (Eds.), Amphibian Biology, vol. 4. Paleontology, the Evolutionary History of Amphibians. Surrey Beatty, Chipping Norton, Australia, pp. 1412–1444.
Miya, M., Nishida, M., 2000. Use of mitogenomic information in teleostean molecular phylogenetics: a tree-based exploration under the maximum-parsimony optimality criterion. Mol. Phylogenet. Evol. 17, 437–455.
Miya, M., Kawaguchi, A., Nishida, M., 2001. Mitogenomic exploration of higher teleostean phylogenies: a case study for moderate-scale evolutionary genomics with 38 newly determined complete mitochondrial DNA sequences. Mol. Biol. Evol. 18, 1993–2009.
Moore, W.S., 1995. Inferring phylogenies from mtDNA variation: Mitochondrial-gene versus nuclear-gene trees. Evolution 49, 718–726.
Moreau, C.S., Bell, C.D., Vila, R., Archibald, S.B., Pierce, N.E., 2006. Phylogeny of the ants: diversification in the age of angiosperms. Science 312, 101–104.
Morescalchi, A., 1975. Chromosome evolution in the caudate amphibia. Evol. Biol. 8, 339–387.
Mueller, R.L., Macey, J.R., Jaekel, M., Wake, D.B., Boore, J.L., 2004. Morphological homoplasy, life history evolution, and historical biogeography of plethodontid salamanders inferred from complete mitochondrial genomes. Proc. Natl. Acad. Sci. USA 101, 13820–13825.
Müller, J., Reisz, R.R., 2005. Four well-constrained calibration points from the vertebrate fossil record for molecular clock estimates. Bioessays 10, 1069–1075.
Murphy, W.J., Eizirik, E., Johnson, W.E., Zhang, Y.P., Ryder, O.A., O'Brien, S.J., 2001. Molecular phylogenetics and the origins of placental mammals. Nature 409, 614–618.
Naylor, B.G., Fox, R.C., 1993. A new ambystomatid salamander, *Dicamptodon antiquus* n. sp. from the Paleocene of Alberta. Can. J. Earth Sci. 30, 814–818.
Posada, D., Crandall, K.A., 1998. MODELTEST: testing the model of DNA substitution. Bioinformatics 14, 817–818.
Rage, J.C., Rocek, Z., 1989. Redescription of *Triadobatrachus massinoti* (Piveteau, 1936), an anuran amphibian from the early Triassic. Palaeont. Abt. A 206, 1–16.
Rannala, B., Yang, Z., 2007. Inferring speciation times under an episodic molecular clock. Syst. Biol. 56, 453–466.
Ree, R.H., Moore, B.R., Webb, C.O., Donoghue, M.J., 2005. A likelihood framework for inferring the evolution of geographic range on phylogenetic trees. Evolution 59, 2299–2311.
Reyes, A., Pesole, G., Saccone, C., 1998. Complete mitochondrial DNA sequence of the fat dormouse, *Glis glis*: further evidence of rodent paraphyly. Mol. Biol. Evol. 15, 499–505.
Reyes, A., Gissi, C., Pesole, G., Catzeflis, F.M., Saccone, C., 2000. Where do rodents fit? Evidence from the complete mitochondrial genome of *Sciurus vulgaris*. Mol. Biol. Evol. 17, 979–983.
Roelants, K., Gower, D.J., Wilkinson, M., Loader, S.P., Biju, S.D., Guillaume, K., Moriau, L., Bossuyt, F., 2007. Global pattern of diversification in the history of modern amphibians. Proc. Natl. Acad. Sci. USA 104, 887–892.
Ronquist, F., 1997. Dispersal-vicariance analysis: a new approach to the quantification of historical biogeography. Syst. Biol. 45, 195–203.
Saccone, C., Giorgi, C.D., Gissi, C., Pesole, G., Reyes, A., 1999. Evolutionary genomics in Metazoa: the mitochondrial DNA as a model system. Gene 238, 195–209.
Samuels, A.K., Weisrock, D.W., Smith, J.J., France, K.J., Walker, J.A., Putta, S., Voss, S.R., 2005. Transcriptional and phylogenetic analysis of five complete ambystomatid salamander mitochondrial genomes. Gene 349, 43–53.
Sanderson, M.J., 2003. R8s: inferring absolute rates of molecular evolution and divergence times in the absence of a molecular clock. Bioinformatics 19, 301–302.
San Mauro, D., Vences, M., Alcobendas, M., Zardoya, R., Meyer, A., 2005. Initial diversification of living amphibians predated the breakup of Pangaea. Am. Nat. 165, 590–599.
Scheltinga, D.M., Jamieson, B.G.M., 2003. The mature spermatozoon. In: Sever, D.M. (Ed.), Reproductive biology and phylogeny of Urodela (Amphibia). NH Science Publishers, Enfield, pp. 203–265.
Sever, D.M., Rania, L.C., Krenz, J.D., 1996. Reproduction of the salamander *Siren intermedia Le Conte* with especial reference to oviducal anatomy and mode of fertilization. J. Morphol. 227, 335–348.
Shimodaira, H., Hasegawa, M., 2001. CONSEL: for assessing the confidence of phylogenetic tree selection. Bioinformatics 17, 1246–1247.
Shimodaira, H., 2002. An approximately unbiased test of phylogenetic tree selection. Syst. Biol. 51, 492–508.
Springer, M.S., DeBry, R.W., Douady, C., Amrine, H.M., Madsen, O., de Jong, W.W., Stanhope, M.J., 2001. Mitochondrial versus nuclear gene sequences in deep-level mammalian phylogeny reconstruction. Mol. Biol. Evol. 18, 132–143.
Steven, S.M., 1999. Earth System History. W.H. Freeman and Company, New York.
Swofford, D.L., 2001. PAUP* : phylogenetic analysis using parsimony (* and other methods), version 4.0b8. Sinauer Associates, Sunderland, Massachusetts.
Thompson, J.D., Gibson, T.J., Plewniak, F., Jeanmougin, F., Higgins, D.G., 1997. The ClustalX windows interface: flexible strategies for multiple sequence alignment aided by quality analysis tools. Nucleic Acids Res. 24, 4876–4882.
Thorne, J.L., Kishino, H., 2002. Divergence time and evolutionary rate estimation with multilocus data. Syst. Biol. 51, 689–702.
Tiffney, B.H., 2000. Geographic and climatic influences on the Cretaceous and Tertiary history of Euramerican floristic similarity. Acta Univ. Carol. Geol. 44, 5–16.
Trontelj, P., Goricki, S., 2003. Monophyly of the family Proteidae (Amphibia: Caudata) tested by phylogenetic analysis of mitochondrial 12S rDNA sequences. Nat. Croat. 12, 113–120.
Vieites, D.R., Min, M.S., Wake, D.B., 2007. Rapid diversification and dispersal during periods of global warming by plethodontid salamanders. Proc. Natl. Acad. Sci. USA 104, 19903–19907.
Vieites, D.R., Zhang, P., Wake, D.B., 2009. Salamanders (Caudata). In: Hedges, S.B., Kumar, S. (Eds.), The Timetree of Life. Oxford University Press, pp. 365–368.
Wang, Y., 2004. A new Mesozoic caudate (*Liaoxitriton daohugoensis* sp. nov.) from Inner Mongolia, China. Chinese Sci. Bull. 49, 858–860.
Weisrock, D.W., Harmon, L.J., Larson, A., 2005. Resolving deep phylogenetic relationships in salamanders: analyses of mitochondrial and nuclear genomic data. Syst. Biol. 54, 758–777.
Wiens, J.J., Bonett, R.M., Chippindale, P.T., 2005. Ontogeny discombobulates phylogeny: paedomorphosis and higher-level salamander relationships. Syst. Biol. 54, 91–110.
Wiens, J.J., 2007. Review of "The amphibian tree of life" by Frost et al.. Quart. Rev. Biol. 82, 55–56.
Wiens, J.J., Kuczynski, C.A., Smith, S.A., Mulcahy, D.G., Sites Jr., J.W., Townsend, T.M., Reeder, T.W., 2008. Branch lengths, support, and congruence: testing the phylogenomic approach with 20 nuclear loci in snakes. Syst. Biol. 57, 420–431.
Xia, X., Xie, Z., 2001. DAMBE: data analysis in molecular biology and evolution. J. Hered. 92, 371–373.
Xia, X., Xie, Z., Salemi, M., Chen, L., Wang, Y., 2003. An index of substitution saturation and its application. Mol. Phylogenet. Evol. 26, 1–7.
Yang, Z., 1997. PAML: A program package for phylogenetic analysis by maximum likelihood. Comput. Appl. Biosci. 13, 555–556.
Yang, Z., Rannala, B., 2006. Bayesian estimation of species divergence times under a molecular clock using multiple fossil calibrations with soft bounds. Mol. Biol. Evol. 23, 212–226.
Zachos, J., Pagani, M., Sloan, L., Thomas, E., Billups, K., 2001. Trends, rhythms, and aberrations in global climate 65 Ma to present. Science 292, 686–693.
Zardoya, R., Meyer, A., 1996. Phylogenetic performance of mitochondrial protein-coding genes in resolving relationships among vertebrates. Mol. Biol. Evol. 13, 933–942.
Zhang, P., Chen, Y.Q., Liu, Y.F., Zhou, H., Qu, L.H., 2003a. The complete mitochondrial genome of the Chinese giant salamander, Andrias davidianus (Amphibia: Caudata). Gene 311, 93–98.
Zhang, P., Chen, Y.Q., Zhou, H., Wang, X.L., Qu, L.H., 2003b. The complete mitochondrial genome of a relic salamander, ranodon sibiricus (Amphibia: Caudata) and implications for amphibian phylogeny. Mol. Phylogenet. Evol. 28, 620–626.
Zhang, P., Zhou, H., Chen, Y.Q., Liu, Y.F., Qu, L.H., 2005. Mitogenomic perspectives on the origin and phylogeny of living amphibians. Syst. Biol. 54, 391–400.
Zhang, P., Chen, Y.Q., Zhou, H., Liu, Y.F., Wang, X.L., Papenfuss, T.J., Wake, D.B., Qu, L.H., 2006. Phylogeny, evolution, and biogeography of Asiatic Salamanders (Hynobiidae). Proc. Natl. Acad. Sci. USA 103, 7360–7365.
Zhang, P., Papenfuss, T.J., Wake, M.H., Qu, L.H., Wake, D.B., 2008. Phylogeny and biogeography of the family Salamandridae (Amphibia: Caudata) inferred from complete mitochondrial genomes. Mol. Phylogenet. Evol. 49, 586–597.